

Warm climate isotopic simulations: What do we learn about interglacial signals in Greenland ice cores?

Louise C. Sime^a, Camille Risi^{bf}, Julia C. Tindall^c, Jesper Sjolte^{dg}, Eric W. Wolff^a, Valérie Masson-Delmotte^e, Emilie Capron^a

^a*British Antarctic Survey, Cambridge, CB3 0ET, U.K.*

^b*Cooperative Institute for Research in Environmental Sciences, University of Colorado, Boulder, U.S.A.*

^c*School of Earth and Environment, University of Leeds, Leeds, LS2 9JT, U.K.*

^d*Niels Bohr Institute, Centre for Ice and Climate, University of Copenhagen, Juliane Maries Vej 30, DK-2100 Copenhagen, Denmark*

^e*Laboratoire des Sciences du Climat et de l'Environnement (UMR 8212 CEA-CNRS-UVSQ), Gif-sur-Yvette, France*

^f*Laboratoire de Météorologie Dynamique (IPSL/CNRS/UPMC), Paris, France*

^g*GeoBiosphere Science Centre, Quaternary Sciences, Lund University, Slvegatan 12, SE-223 62 Lund, Sweden*

Abstract

1 Measurements of last interglacial stable water isotopes in ice cores show
2 that central Greenland $\delta^{18}O$ increased by at least 3 ‰ compared to present
3 day. Attempting to quantify the Greenland interglacial temperature change
4 from these ice core measurements rests on our ability to interpret the sta-
5 ble water isotope content of Greenland snow. Current orbitally driven in-
6 terglacial simulations do not show $\delta^{18}O$ or temperature rises of the correct
7 magnitude, leading to difficulty in using only these experiments to inform our
8 understanding of higher interglacial $\delta^{18}O$. Here, analysis of greenhouse gas
9 warmed simulations from two isotope-enabled general circulation models, in
10 conjunction with a set of last interglacial sea surface observations, indicates a
11 possible explanation for the interglacial $\delta^{18}O$ rise. A reduction in the winter
12 time sea ice concentration around the northern half of Greenland, together
13 with an increase in sea surface temperatures over the same region, is found
14 to be sufficient to drive a > 3 ‰ interglacial enrichment in central Green-
15 land snow. Warm climate $\delta^{18}O$ and δD in precipitation falling on Greenland
16 are shown to be strongly influenced by local sea surface condition changes:
17 local sea surface warming and a shrunken sea ice extent increase the pro-
18 portion of water vapour from local (isotopically enriched) sources, compared

19 to that from distal (isotopically depleted) sources. Precipitation intermit-
20 tency changes, under warmer conditions, leads to geographical variability in
21 the $\delta^{18}O$ against temperature gradients across Greenland. Little sea surface
22 warming around the northern areas of Greenland leads to low $\delta^{18}O$ against
23 temperature gradients (0.1-0.3 ‰ per °C), whilst large sea surface warm-
24 ings in these regions leads to higher gradients (0.3-0.7 ‰ per °C). These
25 gradients imply a wide possible range of present day to interglacial temper-
26 ature increases (4 to >10°C). Thus, we find that uncertainty about local
27 interglacial sea surface conditions, rather than precipitation intermittency
28 changes, may lead to the largest uncertainties in interpreting temperature
29 from Greenland ice cores. We find that interglacial sea surface change obser-
30 vational records are currently insufficient to enable discrimination between
31 these different $\delta^{18}O$ against temperature gradients. In conclusion, further in-
32 formation on interglacial sea surface temperatures and sea ice changes around
33 northern Greenland should indicate whether +5°C during the last interglacial
34 is sufficient to drive the observed ice core $\delta^{18}O$ increase, or whether a larger
35 temperature increases or ice sheet changes are also required to explain the
36 ice core observations.

Keywords: Greenland, interglacials, atmospheric modelling, stable water
isotopes, ice cores

37 1. Introduction

38 Stable water isotope measurements, $\delta^{18}O$ and δD , in polar ice cores pro-
39 vide valuable information on past temperature. A main control on the dis-
40 tribution of $\delta^{18}O$ (and equivalently, for this case, δD) in preserved ice in
41 Greenland is local temperature (Dansgaard, 1964). Thus the stable water
42 isotopic content of ice cores can be used as an indicator of past temperature.

43 Understanding last interglacial temperature across Greenland could help
44 with assessing the impacts of a shrunken Greenland ice sheet (*e.g.* Letreguilly
45 et al., 1991; Chen et al., 2006; Velicogna, 2009; Vinther et al., 2009; Colville
46 et al., 2011), and may offer an opportunity to understand how aspects of
47 the Earth system (*e.g.* sea ice and ocean temperatures) behave in a period of
48 Arctic warmth (*e.g.* Cuffey and Marshall, 2000; Johnsen et al., 2001; NGRIP
49 Project Members, 2004; Masson-Delmotte et al., 2006; Vinther et al., 2009;
50 Turney and Jones, 2010; Masson-Delmotte et al., 2010).

51 The current longest well dated undisturbed Greenland ice core record

52 of $\delta^{18}O$ published is 123 ka long and is from NorthGRIP (NGRIP Project
53 Members, 2004). However the peak of the last interglacial is thought to have
54 occurred between 125 and 130 thousand years before present (ky), most likely
55 at about 126 ky (Otto-Bliesner et al., 2006; Masson-Delmotte et al., 2011).
56 The NorthGRIP record therefore contains no isotopic information from the
57 early part of the last interglacial. The high $\delta^{18}O$ value at 123 ka nevertheless
58 suggests that the temperature in the last interglacial part of the record was
59 substantially warmer than at any time in the Holocene.

60 In order to make the link between climate change and $\delta^{18}O$ responses, it is
61 necessary to understand climatic impacts on $\delta^{18}O$ across Greenland. Green-
62 land $\delta^{18}O$ measurements have been traditionally converted into temperature
63 using the linear relationship (*e.g.* $\delta^{18}O = aT + b$, where T is the surface tem-
64 perature) derived from spatial information (Dansgaard, 1964; Jouzel et al.,
65 1994, 1997). Spatial observations of $\delta^{18}O$ and temperature show a strong lin-
66 ear relationship with a gradient, for inland sites, of about 0.7 to 0.8 ‰ per
67 °C (Johnsen et al., 1995; Sjolte et al., 2011). However, since evaporation
68 conditions, transport pathways, and site elevation changes also effect $\delta^{18}O$,
69 there are many reasons why temporal gradients, and hence the interpretation
70 of temperature shifts through time, may differ from the spatial gradients (see
71 also *e.g.* Dansgaard, 1964; Jouzel et al., 1997; Noone and Simmonds, 2004;
72 Helsen et al., 2007; Schmidt et al., 2007; Sime et al., 2008; Noone, 2008;
73 Cuffey and Paterson, 2010).

74 Alternative information that can be used to help understand how the
75 $\delta^{18}O$ record has varied with past Greenland temperature is available from the
76 temperature profile measured in the borehole (Cuffey et al., 1995; Johnsen
77 et al., 1995; Dahl-Jensen et al., 1998), and from measurements of the isotopic
78 composition of the air trapped in ice (Severinghaus et al., 1998; Severinghaus
79 and Brook, 1999; Capron et al., 2010; Kobashi et al., 2011). The temporal
80 gradients obtained in these studies are generally significantly smaller than the
81 spatial gradients. Values range from 0.23 to 0.55 ‰ per °C, with most values
82 falling around 0.3 ‰ per °C. Interestingly, despite this evidence, papers
83 discussing the last interglacial record have nevertheless generally used the 0.7
84 ‰ per °C gradient (which implies that +3.5 ‰ in $\delta^{18}O$ might be interpreted
85 as equivalent to +5°C shift in temperature) to infer past temperature shifts
86 (*e.g.* NGRIP Project Members, 2004).

87 For a past warmer interglacial climate, where the temperature informa-
88 tion from the borehole and isotopic measurements from trapped air are not
89 available, a possible alternative test of temporal gradients is to calculate $\delta^{18}O$

90 and temperature values over a range of climates using an isotopically enabled
91 general circulation model (GCM) (*e.g.* Jouzel et al., 1994; Sime et al., 2008).
92 For cold climate shifts, the isotopic signal in ice cores in Greenland seem to
93 be more biased towards summer snow (Krinner and Werner, 2003); though
94 it is worth noting that the sign and magnitude of this biasing or precipita-
95 tion intermittency change effect does vary between models. Similar biasing
96 issues also appear to occur in Antarctica under warmer climates (Sime et al.,
97 2009b). Model based results have thus been used as an explanation of low
98 (0.3-0.4 ‰ per °C) $\delta^{18}O$ against temperature gradients for past climate
99 cold-shifts across Greenland (Krinner et al., 1997; Werner et al., 2000).

100 For Greenland, the temperature and isotopic increases simulated across
101 Greenland using an ocean-atmosphere GCM forced only by interglacial or-
102 bital and greenhouse gas forcing are very small; the Masson-Delmotte et al.
103 (2011) isotopic shift amounts to less than 20% of the observed interglacial
104 isotopic shift. This implies that these simulations are not yet in good agree-
105 ment with observational constraints, and that it is difficult to use only these
106 orbitally-driven simulations to help understand interglacial $\delta^{18}O$ in ice cores.
107 Here we therefore complement the Masson-Delmotte et al. (2011) orbital ap-
108 proach with the detailed investigation of isotopic climate simulations warmed
109 by greenhouse gas forcing. In using this method we are not trying to use the
110 greenhouse gas (GHG) driven simulations as a direct analogue for last inter-
111 glacial, rather the approach allows investigation of the isotopic response to
112 patterns of sea surface warming and sea ice change.

113 In overview, the manuscript first compiles last interglacial Greenland iso-
114 topic and Atlantic and Arctic sea surface observations. Secondly, we present
115 a brief discussion of the isotopic models and GHG driven simulations. Third,
116 simulation results are presented in two parts. Present day simulation results
117 are compared to present day Greenland observations, then the warmer simu-
118 lation results are presented and discussed. Fourth, we consider what we can
119 learn from the warmer simulation results, in the context of last interglacial
120 sea surface observations, about the interpretation of last interglacial ice in
121 Greenland cores. Finally, the last section summarises our findings and draws
122 together some conclusions.

123 2. Interglacial observations from Greenland and its surrounding 124 region

125 In comparison with present day, Holocene, or even last glacial condi-
126 tions, the amount of information about the last interglacial peak (around
127 125-130 ky) is rather limited (*e.g.* Johnsen et al., 2001; MARGO Project
128 Members, 2009; Leduc et al., 2010). An overview of the currently available
129 last interglacial observations for Greenland ice cores, and for near Greenland
130 sea surface condition observations, is provided below. Note, observations of
131 present day temperature, accumulation, and $\delta^{18}O$ from ice core tops and
132 other surface sites across Greenland are provided in Appendix B.

133 2.1. Interglacial Greenland ice core observations:

134 There is currently no complete record of the last interglacial from Green-
135 land ice cores. However, there are four publicly available Greenland stable
136 water isotope ice core records that may feature some last interglacial ice (Fig.
137 1b). The $\delta^{18}O$ isotopic records from NGRIP, GRIP, Renland, DYE3, and
138 Camp Century show similar variations over the majority of the last glacial
139 period. This strongly suggests that the upper parts of these cores depict
140 continuous undisturbed climatic records. However, the lack of agreement
141 between their bottom parts implies that stratigraphic disturbances perturb
142 their respective depth-age relationships. See Fig. 1 for positions and $\delta^{18}O$
143 records. Fig. 1a also shows the maximum difference in $\delta^{18}O$ between present
144 day (0-3 ky average) and the ‘last interglacial’ maximum (the highest value
145 in Fig. 1b which occurs before 100 ky).

146 Of the available Greenland ice core records, NGRIP is the only site which
147 provides a continuous undisturbed climatic record back to the last inter-
148 glacial. However, bedrock was reached at 3085 m and the deepest ice is
149 thought to be 123 ky old (NGRIP Project Members, 2004; Landais et al.,
150 2005). Thus, the NGRIP ice core probably does not record the maximum
151 peak of the last interglacial. At GRIP the lowest 10% of the core, older than
152 110 ky, has a disturbed stratigraphy (Landais et al., 2003; Suwa et al., 2006).
153 While the observed $\delta^{18}O$ at the bottom of the core suggests the presence
154 of interglacial ice (Fig. 1), there is doubt whether peak interglacial $\delta^{18}O$
155 values are represented (GRIP Project Members, 1993; Johnsen et al., 2001;
156 Suwa et al., 2006). The Renland record has a depth-age model only until
157 60 ky (Svensson et al., 2008). For simplicity, the isotopically lightest near
158 bed Renland ice is placed at 123 ky, however it is likely that this also does

159 not represent a peak interglacial value. For DYE3, there is also no available
160 depth-age model for the deep ice, and evidence of silt in this core bottom
161 ice means that the maximum old ice $\delta^{18}O$ could be representative of some-
162 thing other than precipitation directly over the site (Langway et al., 1985;
163 Johnsen et al., 2001). A fifth Greenland ice core $\delta^{18}O$ record was obtained
164 from Camp Century in north west Greenland around 1972 (Johnsen et al.,
165 1972). Although we do not have the measurements available to place Camp
166 Century values on Fig. 1b, this site also appears to contain some last inter-
167 glacial ice (Johnsen et al., 2001). The magnitude of the present day to last
168 interglacial Camp Century peak changes in $\delta^{18}O$ seems similar to those from
169 the more central (NGRIP, GRIP, and Renland) sites, at between + 3 and +
170 5 ‰ (Johnsen et al., 2001; NGRIP Project Members, 2004).

171 A conservative summary of the available $\delta^{18}O$ records is simply that be-
172 tween the present day and the peak of the last warm interglacial (somewhere
173 between 125-130 ky), there was an increase in $\delta^{18}O$ of at least 3 ‰ in cen-
174 tral and north-western Greenland. For southern and eastern Greenland $\delta^{18}O$
175 variations suggest that last interglacial values were also higher (Fig. 1b), but
176 the values seem currently too uncertain to be used as individual quantitative
177 observational constraints.

178 *2.2. Interglacial sea surface condition observations:*

179 Available observations used to reconstruct maximum last interglacial sea
180 surface temperatures from various paleoclimatic archives were compiled by
181 Turney and Jones (2010). A compilation considering the maximum temper-
182 ature peak may not be reflective of any one single last interglacial climatic
183 period (Lang and Wolff, 2010; Govin et al., 2012). Thus there is doubt over
184 whether these peak reconstructed sea surface interglacial temperatures are
185 co-incident everywhere across the Northern Hemisphere. Table 2 presents
186 the rather sparse set of available qualitative observations of last interglacial
187 sea ice changes from across the Northern Hemisphere. Please see Section 5
188 for analysis and discussion of these last interglacial sea surface temperature
189 and sea ice observational constraints.

190 **3. Isotopic Modelling**

191 Two sets of atmospheric general circulation model (AGCM) simulations
192 are used in this study of climate and isotopes in precipitation over Green-
193 land (Table 1). We wish to simulate the observed magnitude of the last in-

194 interglacial Greenland $\delta^{18}O$ shift. Since an orbitally driven approach appears
195 to fail to drive the correct magnitude of $\delta^{18}O$ increase (Masson-Delmotte
196 et al., 2011), we use GHG-forced simulations from different coupled models,
197 which feature contrasting sea surface temperature responses. We are not
198 trying to use these GHG driven simulations as a direct analogue for last in-
199 terglacial, nevertheless the approach allows insight into the interpretation of
200 interglacial isotopic changes across Greenland. One set of experiments uses
201 the isotopically enabled HadAM3 atmospheric model, and one uses the iso-
202 topically enabled atmospheric LMDZ4 model. Using two models allows us
203 to also investigate whether differing atmospheric physics between the models
204 affects our findings.

205 3.1. The use of greenhouse gas forced simulations:

206 Our goal here is to investigate the isotopic response to different patterns
207 of warming, which may be of a magnitude similar to those of the last in-
208 terglacial. It is useful if these patterns are diverse; diversity increases the
209 likelihood that we encompass the last interglacial pattern.

210 Our warm climate simulations are driven by greenhouse gas (GHG),
211 rather than interglacial orbital forcing. Note, as in Sime et al. (2008) CO_2
212 and GHG driven warming are used interchangeably *i.e.* where CO_2 is writ-
213 ten, we wish to imply CO_2 equivalent GHG forcing. The use of the GHG
214 warming, rather than orbital forcing, as noted in the introduction, is done
215 for three main reasons. Firstly, the amount of annual mean warming across
216 Greenland in the Masson-Delmotte et al. (2011) orbitally forced simulation
217 is very small ($+0.9^\circ C$ at 126 ky). Although the interglacial orbitally-driven
218 summer warming, of close to $5^\circ C$, agrees with some available summer obser-
219 vations (CAPE Project Members, 2006), the annual mean warming of $0.9^\circ C$
220 is very small (less than 20%) compared with previous temperature recon-
221 structions (NGRIP Project Members, 2004).

222 Secondly, the Greenland isotopic shift in the orbitally forced simulations
223 is very small, at around $+0.1$ to $+0.5$ ‰ of $\delta^{18}O$ (Masson-Delmotte et al.,
224 2011). This simulated shift amounts to less than 20% of the observed inter-
225 glacial isotopic shift (Fig. 1). The small orbitally forced interglacial Green-
226 land temperature and isotopic shifts lead to difficulty in interpreting tem-
227 poral $\delta^{18}O$ against temperature gradients. This is because the geographical
228 variability in temporal gradients (see also Sime et al., 2009b) between these
229 orbital-interglacial and present day experiments is large (two orders of mag-
230 nitude larger than in the GHG forcing, see section 4.5) in these experiments

231 (not shown). Effectively, the low climate signal to climate noise ratio means
232 that interpretation of the climate-isotope signal is extremely difficult.

233 A third reason it is useful to focus on the GHG forced experiments is the
234 large differences between the coupled model sea surface boundary changes
235 (see Section 4.2 for details and results). Many differences in coupled model
236 results can be attributed to the difficulty associated with modelling oceans
237 during non-present day climate periods: for example, present parameteri-
238 sations of ocean mixing may mean that current ocean models are not well
239 suited to simulating climate periods when the ocean is in a different state
240 (Wunsch, 2003; Watson and Naveira Garabato, 2006). Additionally, sea ice is
241 quite poorly represented leading to large biases in high latitude results (*e.g.*
242 Stroeve et al., 2007). These known modelling problems may contribute to
243 the cold and low $\delta^{18}O$ biases in the Masson-Delmotte et al. (2011) simulated
244 interglacial climate. However, here these deficiencies are turned to advan-
245 tage. The HadCM3 and IPSL sea surface differences (mainly due to ocean
246 and sea ice model differences) enable examination of the impact of different
247 warm climate sea surface boundary changes on atmospheric simulations.

248 *3.2. The use of two isotopic AGCMs:*

249 The isotopically enabled AGCMs HadAM3 (isotopic version 1.0, unified
250 model version 4.5) and LMDZ4 both have a regular latitude longitude grid,
251 with a resolution of $2.5^\circ \times 3.75^\circ$, and 19 hybrid coordinate levels in the
252 vertical (Pope et al., 2000; Risi et al., 2010). Tindall et al. (2009) and Risi
253 et al. (2010) present details of the stable water isotopic submodels that were
254 incorporated into HadAM3 and LMDZ4, respectively. The use of two sepa-
255 rate atmospheric isotopic models is helpful for checking whether our results
256 are model specific.

257 *3.3. The isotopic simulations:*

258 The HadAM3 and LMDZ4 control isotopic simulations are based on sim-
259 ilar sets of present day sea surface observations (Table 1). The present day
260 period is used as a control because we can test these simulation results against
261 a set of present day Greenland snow $\delta^{18}O$ observations.

262 For the warmer than present day simulations, coupled ocean-atmosphere
263 versions (HadCM3 and IPSL version CM4) of the respective AGCM are used
264 to simulate warmer than present day climates. The main warmer simulations
265 are driven by similar GHG forcings. Additional very warm simulations driven

266 by larger GHG forcings are also used. Two additional experiments also simu-
267 late the individual effects of the warmer sea surface temperatures (SST) and
268 sea ice changes (SeaIce).

269 The sea surface temperature anomalies from each coupled model simula-
270 tion are applied to the control sea surface temperatures. The atmospheric
271 only, but isotopically enabled, version of the AGCM is then run. This use of
272 sea surface temperature anomalies reduces the impact of known model errors
273 (Krinner et al., 2008; Sime et al., 2008; Masson-Delmotte et al., 2011). All
274 the simulations use fixed (present day) Greenland ice sheet elevations. See
275 Appendix A for more detail on the simulations.

276 4. Isotopic simulation results

277 Firstly, a check of the HadAM3 and LMDZ4 present day simulation re-
278 sults is presented. This is useful to help assess the validity of model-data com-
279 parisons. To help understand what aspects of the warmer climate changes
280 drive the isotopic changes, analysis of isotopic and climatic changes between
281 the present day and warmer simulations is then presented. The following
282 discussion section brings the model analysis together with observational con-
283 straints, and provides an overview of climate insights gleaned from the anal-
284 ysis.

285 4.1. The present day simulation of Greenland ice sheet climate

286 Here a brief overview of the model climatology and isotopic results over
287 Greenland is given. See Appendix B for a more detailed comparison between
288 available observations and present day simulation values (using co-located
289 model results).

290 Table 3 provides present day simulation results using the Masson-Delmotte
291 et al. (2006, 2011) definition of central Greenland *i.e.* using all points higher
292 than 1300 m. Using this >1300 m definition, present day central Greenland
293 HadAM3 temperatures are -24.0°C whilst LMDZ4 values are -18.8°C (Fig.
294 2a and 3a). Annual mean precipitation across the whole central Greenland
295 region for the HadAM3 simulation is 325.8 kg m⁻² yr⁻¹, the LMDZ4 re-
296 sults are wetter at 454.0 kg m⁻² yr⁻¹ (Fig. 2b and 3b). Both HadAM3
297 and LMDZ4 show that the overall geographical pattern of observations and
298 simulation results compare quite well (Fig. 2ab and 3ab). HadAM3 tem-
299 perature and precipitation value are likely more reflective of the observed
300 Greenland climate than LMDZ4 (Appendix B), but in common with other

301 models (Sjolte et al., 2011), the simulated precipitation in both models in
302 southern Greenland is too high (*e.g.* Burgess et al., 2010). Like some other
303 isotopic model simulations of Greenland (*e.g.* Hoffmann and Heimann, 1998;
304 Sjolte et al., 2011), the annual mean isotopic values of the precipitation, in
305 HadAM3 and LMDZ4, are heavier than the observations (Fig. 2c and 3c).
306 This could be related to a warm bias (Sjolte et al., 2011), and possibly also
307 some difficulties in the accurate simulation of seasonal cycles (Appendix B).
308 In general, despite a reasonable orographic representation of central Green-
309 land (Fig. 2f and 3f) and reasonable simulated precipitation, differences in
310 model-observation seasonality and $\delta^{18}O$ do suggest that the origin and path-
311 ways of water to Greenland are, as for other models, also probably not fully
312 accurate for either HadAM3 or LMDZ4.

313 *4.2. Warmer climate simulation results for Greenland.*

314 Here, changes between the present day and main warmer simulations are
315 presented. The HadAM3 SRES A1B and A2 simulations are differenced to
316 the HadAM3 present day simulations. The LMDZ4 CO₂ × 2 and 4 simula-
317 tions are differenced against the LMDZ4 present day simulation. See Table
318 3 for a summary of simulated mean annual central Greenland changes.

319 *4.2.1. Mean annual changes:*

320 Fig. 4 shows $\delta^{18}O$ changes between the HadAM3 and LMDZ4 warmer
321 and present day simulations (left hand panels). The central Greenland $\delta^{18}O$
322 changes for HadAM3 A1B simulations (Fig. 4ab) and for the warmest
323 LMDZ4 CO₂ × 4 simulation (Fig. 4gh) both show changes of +3.6 and
324 +1.8 ‰ in $\delta^{18}O$, respectively. These values are comparable to the observed
325 interglacial $\delta^{18}O$ increase in central Greenland (Fig. 1).

326 For the HadAM3 SRES A1B simulation, mean annual results (central
327 Greenland >1300 m), mean central Greenland temperature and precipitation
328 changes between the present day and warmer simulation are: +4.7°C and +93
329 kg m⁻² yr⁻¹, and an enrichment in $\delta^{18}O$ of +3.6 ‰. For the warmer HadAM3
330 SRES A2 simulation, mean central Greenland temperature and precipitation
331 changes by: +5.4°C and +117.1 kg m⁻² yr⁻¹, and an enrichment in $\delta^{18}O$ of
332 +3.9 ‰ occurs. Both of the warmer HadAM3 simulations shown in Fig.
333 4 display quite large changes in the isotopic values. The spatial pattern of
334 changes in $\delta^{18}O$ is closely related to changes in temperature and precipitation
335 for these simulations (Fig. 4).

336 For the LMDZ4 CO₂ × 2 simulation, mean central Greenland temper-
337 ature and precipitation changes are: +3.3°C and +74.1 kg m⁻² yr⁻¹, but
338 the enrichment in δ¹⁸O is quite small at 0.31 ‰. For the warmer LMDZ4
339 CO₂ × 4 simulation mean central Greenland temperature and precipita-
340 tion changes are: +7.3°C and +176.1 kg m⁻² yr⁻¹ in precipitation, with a
341 larger enrichment in δ¹⁸O of +1.8 ‰. So, although the temperature and
342 precipitation changes for these LMDZ4 simulations are comparable to the
343 HadAM3 changes, the LMDZ4 simulations feature smaller isotopic changes.
344 The d-excess changes for LMDZ4, like the δ¹⁸O changes, are also smaller
345 than those associated with the HadAM3 simulations (Fig. 4).

346 It is difficult to interpret the d-excess results. HadAM3 and LMDZ each
347 use a slightly different representation of micro-scale cloud physics (Tindall
348 et al., 2009; Risi et al., 2010). This difference in supersaturation tuning
349 has little impact on either first order δ¹⁸O or δD, but it does affect second
350 order d-excess (Schmidt et al., 2007; Werner et al., 2011). Better model
351 representations of these aspects of micro-scale cloud physics would be helpful
352 in allowing a more insightful analysis of d-excess observations (Noone and
353 Sturm, 2010).

354 The pattern of temperature, precipitation, and δ¹⁸O changes suggest a
355 relationship between the climate driven isotopic response over Greenland and
356 the sea surface conditions in the vicinity of Greenland (Fig. 4). The HadAM3
357 simulations tend to show a larger degree of warming, precipitation change,
358 and isotopic change in the central northern regions of Greenland, particularly
359 towards the east. This ties in with larger sea surface temperature and sea
360 ice changes towards the north and east. Changes in d-excess (Fig. 4, right
361 panels, shaded over Greenland) also show similarity to temperature and δ¹⁸O
362 changes (Fig. 4, left panels, contoured and shaded) and a weaker similarity
363 to precipitation changes.

364 For every model simulation, southern regions of Greenland show smaller
365 changes in temperature, precipitation, δ¹⁸O, and d-excess (Fig. 4). This is
366 likely related to the relatively small changes in sea surface conditions sur-
367 rounding this region of Greenland.

368 4.2.2. Seasonal changes:

369 There is a strong seasonal relationship between changes in temperature
370 and δ¹⁸O (Fig. 5). The monthly changes in precipitation are also visually
371 closely tied to the temperature changes, but monthly d-excess shows a dif-
372 ferent pattern. Fig. 6 shows a selection of possible predictors of isotopic

373 changes. The subsequent section examines causation, however here we sim-
374 ply regress the anomalous monthly $\delta^{18}O$ and d-excess (Fig. 5) on pairs of
375 these possible predictors (Fig. 6) to examine correlations on the seasonal
376 timescale. HadAM3 monthly $\delta^{18}O$ changes are strongly correlated with local
377 SST and evaporation changes (up to 86% of monthly $\delta^{18}O$ variance is ex-
378 plained). LMDZ4 monthly $\delta^{18}O$ changes are better correlated with broader
379 North Atlantic region changes in evaporation and sea surface conditions (up
380 to 62% of monthly $\delta^{18}O$ variance explained). The monthly d-excess anoma-
381 lies for LMDZ4 are strongly correlated with local evaporation and higher
382 sea surface temperature (up to 85% of variance explained), whilst HadAM3
383 d-excess is more closely related to wider North Atlantic evaporation and sea
384 ice changes (up to 67% of variance explained). In summary, whilst HadAM3
385 and LMDZ4 isotopes seem to respond slightly differently to different seasonal
386 climate changes, in both models $\delta^{18}O$ and d-excess tend to respond most
387 strongly to: local temperature; sea surface temperature; sea ice changes; and
388 evaporation.

389 *4.3. The impact of surface conditions and source effects*

390 Section 4.2 suggests that sea surface condition changes are key to under-
391 standing changes in $\delta^{18}O$ in Greenland snow. Here, additional HadAM3 sen-
392 sitivity simulations and LMDZ4 source tracking simulations are presented to
393 help clarify mechanisms. Two sensitivity simulations were performed where
394 the sea surface temperatures and sea ice changes were applied individually
395 (Table 1). The differences between Fig. 7a and Fig. 7c suggest that the
396 applied sea surface temperature changes tend to raise the inland tempera-
397 tures and $\delta^{18}O$ values more than the sea ice changes do, but Fig. 7b and
398 Fig. 7d (contours) suggests that in the north-east Greenland the precipita-
399 tion changes are approximately equally dependent on both the sea surface
400 temperature and sea ice changes.

401 Comparison of the HadAM3 SeaIce (warm climate sea ice retreat but no
402 sea surface temperature change, Fig. 7cd) and LMDZ4 $CO_2 \times 2$ and \times
403 4 results (Fig. 4efgh) shows several similarities. The sea surface condition
404 changes around Greenland in LMDZ4 $CO_2 \times 2$ and $CO_2 \times 4$ are closer to
405 HadAM3 SeaIce simulation than the A1B simulation; the sea surface temper-
406 atures change not much (or not at all) in each of these LMDZ4 experimen-
407 ts around the northern edge of Greenland. A substantial loss of sea ice around
408 Greenland however does occur in each of these simulations. As a result,
409 the isotopic responses in central Greenland for both LMDZ4 simulations are

410 similar to the HadAM3 SeaIce sensitivity simulation. Appendix C confirms
411 that these sea surface conditions are the main drivers of the model isotopic
412 response; differences in model physics are relatively unimportant. In each
413 case, the $\delta^{18}O$ enrichment (Fig. 4e), the d-excess change patterns (Fig. 4fh),
414 and the $\delta^{18}O$ - against temperature gradients (see Table 3) are similar. This
415 is particularly apparent when comparing the HadAM3 SeaIce and LMDZ4
416 $CO_2 \times 4$ model simulations.

417 The difference between Fig. 4ab and Fig. 7ef indicates that the Fig. 4ab
418 pattern and magnitude of changes in temperature, precipitation, $\delta^{18}O$, and
419 d-excess can neither be fully replicated by simulations which apply the sea
420 surface temperature changes (Fig. 7ab) nor just the sea ice changes (Fig.
421 7cd): applying the changes in sea surface temperature or sea ice separately
422 is not equivalent to applying both changes simultaneously. The isotopic
423 response (shading over Greenland) for the SST + SeaIce is smaller than for
424 SST and SeaIce changes combined (*i.e.* the A1B Fig. 4ab results). This
425 indicates that there are some non-linearities in the response of Greenland
426 temperature, precipitation, $\delta^{18}O$, and d-excess to reductions in sea ice and
427 sea surface temperature increases.

428 4.4. Precipitation source effects on isotopic values:

429 Whilst Section 4.2 and 4.3 both emphasise that sea surface temperature
430 and sea ice changes strongly affect isotopic changes over Greenland, Section
431 4.3 also indicates that joint (non-linear) effects of sea surface temperature
432 and sea ice changes together drive larger isotopic changes. One of the possible
433 ways in which non-linear behaviour may impact on $\delta^{18}O$ is through
434 sea surface evaporation effects (Masson-Delmotte et al., 2005). For high latitudes,
435 Noone (2008) shows that if the proportion of precipitation vapour
436 sourced from local sea surface local regions increases, isotopic enrichment of
437 precipitation tends to occur. Source changes therefore can change the isotopic
438 composition of Greenland snow (*e.g.* Hoffmann and Heimann, 1997;
439 Noone, 2008; Masson-Delmotte et al., 2011).

440 Source tracking is useful in allowing the origin of precipitation over Green-
441 land to be ascertained (see Appendix C for technical details). The exper-
442 iments outlined in 3.3.2 are therefore also run with the LMDZ4 model us-
443 ing the source-tracking feature (see Appendix D for details). Precipitation
444 sources over Greenland are divided into three regions: high latitude (sea
445 surface north of $50^\circ N$); mid-low latitude (sea surface south of $50^\circ N$); and

446 continental (from all continental regions). Using the same central Green-
447 land definition as in Section 4.1 above, the source tracking results indicate
448 that most present day central Greenland precipitation is sourced from mid-
449 low latitude regions (51 %), with lesser amounts originating from more local
450 high-latitude (19%) and continental (30%) regions (Table 4). Table 4 in-
451 dicates that mid-low latitude and continental region sourced precipitation
452 tends have a depleted $\delta^{18}O$ value, of around -30 to -40 ‰, whilst the (lo-
453 cal) high-latitude sourced precipitation is substantially more enriched, at
454 around $+2$ to $+5$ ‰.

455 Analysis of results for these additional source tracked simulations shows
456 quite different changes in precipitation sources. The strong sea surface tem-
457 perature warming north of Greenland in HadCM3 generates a substantial
458 (approx 15%) increase in the percentage of high-latitude precipitation across
459 northern Greenland (Fig. 8a). In contrast to this, the strong mid-low latitude
460 sea surface temperature warming and much smaller changes around Green-
461 land produced by IPSL, leads to a large percentage reduction (approx -15%)
462 in high-latitude precipitation across the whole of Greenland. Precipitation
463 in this simulation instead becomes more influenced by mid-low latitude and
464 continentally sourced precipitation. This difference between the two model
465 simulations is important because it means more distal $\delta^{18}O$ depleted vapour
466 is present in the warmer LMDZ4-IPSL simulations. This will tend to deplete
467 $\delta^{18}O$ value in snow. Whereas for HadAM3-HadCM3, the larger proportion
468 of more local high-latitude vapour across northern Greenland tends to enrich
469 the simulated warmer climate $\delta^{18}O$ values.

470 4.5. Isotope against temperature gradients

471 Despite reasonable similarity in the amount of warming across the AGCM
472 simulations, there is a wide range of temporal $\delta^{18}O$ against temperature gra-
473 dients (Table 3). The HadAM3 simulations yield mean central Greenland
474 gradients of 0.76 and 0.71 ‰ per °C for the A1B and A2 simulations, re-
475 spectively. For LMDZ4, the CO2 $\times 4$ simulation gradient is much lower at
476 0.25 ‰ per °C.

477 In addition to the mean gradient differences between the simulations, it is
478 also of interest to look at what causes geographical variability in the temper-
479 ature against $\delta^{18}O$ relationship across Greenland. Since $\delta^{18}O$ is recorded in
480 precipitation, and is therefore ‘precipitation-weighted’, we also briefly com-
481 pare $\delta^{18}O$ change with precipitation-weighted surface temperature change
482 for each location. Various authors (*e.g.* Krinner et al., 1997; Werner and

483 Heimann, 2002; Krinner and Werner, 2003; Sime et al., 2008, 2009a) have
484 shown that precipitation weighted temperature changes can deviate signifi-
485 cantly from temperature changes. Geographical differences between temper-
486 ature and precipitation weighed temperature anomalies can be important for
487 understanding geographical variations in temporal $\delta^{18}O$ against temperature
488 gradients (Sime et al., 2009b). The weighting is done here using daily precipi-
489 tation and temperature values. See Sime et al. (2008) for details of the calcu-
490 lation. (The difference between temperature and precipitation weighted tem-
491 perature is sometimes called ‘precipitation biasing’.) Additional checks using
492 a subset LMDZ4 results, provided in Appendix C, confirm these HadAM3
493 results also apply to LMDZ4.

494 Fig. 9 shows the $\delta^{18}O$ against temperature gradients for each model sim-
495 ulation (shaded). For the HadAM3 simulations, the contours show the as-
496 sociated changes in precipitation biasing. Each model simulation shows geo-
497 graphical variability in the $\delta^{18}O$ against temperature gradient. The available
498 HadAM3 and LMDZ4 (Appendix C) precipitation biasing results suggest
499 that much of this geographical variability is due to geographical-climate vari-
500 ability in precipitation intermittency (Fig. 9abef). Additional continental-
501 scale geographical variability is also driven by local sea surface condition
502 control of $\delta^{18}O$ (see Fig. 4, and previous sections).

503 In summary, whilst there is some Greenland geographical variability within
504 the simulations due to precipitation intermittency changes, the central Green-
505 land isotopic against temperature gradient differences is also driven by sea
506 surface condition (precipitation source) changes. The overall tendency is
507 for gradients, where substantial sea surface warming occurs north of Green-
508 land (HadAM3 A1B and A2), to be about twice those where no substantial
509 warming occurs (LMDZ4 CO2 \times 2 and 4, and HadAM3 SeaIce).

510 **5. What can we learn about the interpretation Greenland ice cores** 511 **from these simulations?**

512 Here we consider what is learned about the interpretation of ice core
513 measurements from these results. Sections 4.2 to 4.5 indicate sea surface
514 condition changes exert significant control over isotopes recorded in Green-
515 land ice cores. With that in mind, here we first provide an overview of the
516 agreement between sea surface condition observations, and our warmer simu-
517 lations, for the last interglacial. Implications and possible future studies are
518 then discussed.

519 *5.1. Previous warmer than present day sea surface temperature and sea ice*
520 *changes*

521 The Turney and Jones (2010) compilation of sea surface temperature
522 observations are shown in Fig. 10 (square symbols). These Turney and
523 Jones (2010) observations support the idea that maximum last interglacial
524 sea surface temperature anomalies were larger at higher latitudes (*e.g.* Leduc
525 et al., 2010). Additionally, the available interglacial Arctic sea ice indicators
526 (Table 2) suggest that the minimum last interglacial sea ice concentration
527 and (or) extent was reduced compared to the present day (Fig. 10, round
528 symbols).

529 Observations of last interglacial sea ice concentration or extent reductions
530 are sparse and are not quantitative. The two observations agree with all of
531 the simulated warmer climate sea ice concentration reductions (Fig. 4 and
532 10). A more detailed comparison with the simulated results is not possible
533 with these data. There are more Turney and Jones (2010) observations of
534 maximum last interglacial sea surface temperature changes (Fig. 10). All
535 of the available observations are over plotted on HadAM3 SRES A1B (Fig.
536 10a) and LMDZ4 CO₂ × 4 (Fig. 10b) sea surface temperature changes.
537 Fig. 10 shows that both sets of sea surface temperature changes agree with
538 the broad pattern of observations, with larger maximum last interglacial
539 sea surface temperature anomalies at higher latitudes. However, beyond
540 this agreement, rather like the sea ice observations, there is a lack of last
541 interglacial observations in critical regions particularly north of Greenland.
542 HadAM3 and LMDZ4 sea surface changes are quite different in these regions.
543 However a lack of sea surface temperature observations north of 72°N means
544 these simulation differences cannot be assessed.

545 *5.2. How could the interpretation last interglacial elevation and temperature*
546 *changes from $\delta^{18}O$ be improved?*

547 In addition to the last interglacial temperature reconstruction problem,
548 there has been interest in whether isotopic ice core records can also be used to
549 help reconstruct the elevation of past Greenland ice sheet core sites (Vinther
550 et al., 2009; Masson-Delmotte et al., 2011). This would help with assessing
551 the past and possible future impact of such changes on the ice sheet (*e.g.* Le-
552 treguilly et al., 1991; Cuffey and Marshall, 2000; Chen et al., 2006; Velicogna,
553 2009; van de Berg et al., 2011).

554 To aid these future interpretations of interglacial ice $\delta^{18}O$, isotopic mod-
555 elling studies which use varying Greenland icesheet morphologies would be

556 very useful. Other changes which should also be examined include directly
557 orbitally driven insolation effects. For example, radiation driven impacts
558 on the hydrological cycle, and hence on Greenland $\delta^{18}O$ should be clarified
559 (Masson-Delmotte et al., 2011). Interglacial vegetation growth associated
560 with any reduction in the Greenland icesheet also likely has an impact on
561 Greenland $\delta^{18}O$ (Schurgers et al., 2007; Masson-Delmotte et al., 2011). In
562 addition to these possible single attribute modelling studies, fully coupled
563 ocean-atmosphere-seaice-vegetation model studies would also be of value.
564 For example, a reduced interglacial ice sheet could decrease ice core site ele-
565 vations, increase Greenland vegetation, change local atmospheric circulation,
566 and effect sea ice. Thus fully coupled model runs will also be necessary if we
567 wish to achieve the best possible simulation of last interglacial isotopes across
568 Greenland. However, in the meantime, it is likely that attribution studies
569 focussing on single aspects of these problems may be especially helpful in
570 terms of developing our understanding of the critical processes.

571 Finally we note that our findings suggest that the reconstruction of past
572 interglacial ice sheet elevations will also require additional sea surface temper-
573 ature constraints. These additional data would be very helpful in reducing
574 the uncertainties on a joint interglacial reconstruction of temperature and
575 elevation changes from $\delta^{18}O$.

576 6. Summary and conclusions

577 It is of considerable interest to the climate community to better under-
578 stand isotopic ice core records from Greenland; particularly from the past
579 warm interglacial maxima (around 125-130 ky). Five Greenland stable wa-
580 ter isotope ice core records suggest that between the present day and the
581 peak of the last warm interglacial, there was an increase in $\delta^{18}O$ of at least 3
582 ‰ in central and north-western Greenland. There were also likely increases
583 in southern and eastern Greenland. The use of isotopically enabled general
584 circulation models is therefore of value to the ice core and ice sheet commu-
585 nity. With this in mind, two sets of isotopically enabled atmospheric general
586 circulation model simulations, applying the HadAM3 and LMDZ4 models,
587 were used to investigate warm climate changes (Sime et al., 2008, 2009b;
588 Tindall et al., 2009; Risi et al., 2010). In both cases, warmer than present
589 day simulations were generated by applying greenhouse gas forced patterns of
590 sea surface temperature and sea ice change to the models (Sime et al., 2008;
591 Masson-Delmotte et al., 2011). Because traditional orbitally driven simu-

592 lations show less than 20% of the observed $\delta^{18}O$ and temperature change,
593 interpretation of the interglacial $\delta^{18}O$ rise from these traditional simulations
594 is difficult. The greenhouse gas warmed approach is therefore a useful com-
595 plement to the orbital approach, and has here highlighted a possible driver
596 for the interglacial rise in Greenland $\delta^{18}O$.

597 In terms of the models, we have shown that the HadAM3 and LMDZ4 iso-
598 topic responses to sea surface condition changes are very similar (Appendix
599 C), suggesting that any differences in inter-model physics are not a signifi-
600 cant factor in our results. The central Greenland $\delta^{18}O$ changes for warmer
601 HadAM3 simulations and for the warmest LMDZ4 simulation both show in-
602 creases in $\delta^{18}O$ that are commensurate with the observed interglacial rise. A
603 temperature increase of $+4.7^\circ\text{C}$ for HadAM3 is associated with a rise of 3.6
604 ‰ in $\delta^{18}O$. A temperature increase of $+7.3^\circ\text{C}$ for LMDZ4 is associated with
605 a rise of 1.8 ‰ in $\delta^{18}O$. Our simulations show smaller changes in tempera-
606 ture, precipitation, $\delta^{18}O$, and d-excess in southern regions of Greenland, and
607 larger changes in central eastern and northern regions of Greenland.

608 We find that understanding sea surface condition changes is key to un-
609 derstanding Greenland isotopic changes. This is largely because sea surface
610 changes drive differences in precipitation sources, which affect $\delta^{18}O$ values
611 over Greenland. Precipitation sourced from local high-latitude regions is en-
612 riched in $\delta^{18}O$. Increasing (decreasing) the proportion of locally source pre-
613 cipitation therefore raises (lowers) $\delta^{18}O$ in Greenland snow. For the HadAM3
614 warm climate simulations, evaporation changes tend to be strongly positive
615 over the northerly areas around Greenland, due to the combined effect of re-
616 duced sea ice and strongly increased sea surface temperatures. This leads to
617 substantially more local ($\delta^{18}O$ enriched) precipitation falling over northern
618 Greenland. The LMDZ4 simulations feature stronger sea surface temperature
619 increases south of 50°N and little change around Greenland. This leads to a
620 higher proportion of warm climate ($\delta^{18}O$ depleted) distally sourced Green-
621 land precipitation. For this reason, the LMDZ4 $\delta^{18}O$ changes over Greenland
622 are much smaller than those in HadAM3, even when Greenland temperature
623 increases are similar. These differences in HadAM3 and LMDZ4 sea surface
624 temperature forcings lead the HadAM3 $\delta^{18}O$ against temperature gradients
625 to be about twice the magnitude of LMDZ4 gradients. Given that during
626 colder than present day climate periods, $\delta^{18}O$ was more likely sourced from
627 distal (depleted) sources (Masson-Delmotte et al., 2005), a warm climate
628 change towards more locally sourced vapour during the last interglacial may
629 be more likely.

630 We show there are some non-linearities in the response of Greenland tem-
631 perature and $\delta^{18}O$ to reductions in sea ice and sea surface temperature in-
632 creases: applying changes in sea surface temperature or sea ice separately is
633 not equivalent to applying both changes simultaneously. While $\delta^{18}O$ source
634 effects explain the differences between the simulations, we also find that
635 changes in precipitation intermittency explain large geographical differences
636 in the relationship between $\delta^{18}O$ and temperature across Greenland.

637 The Turney and Jones (2010) last interglacial sea surface temperature
638 change dataset lacks observations from around northern Greenland. This
639 means that these observations do not tell us which of the sets of isotopic
640 model simulation results better resembles last interglacial sea surface condi-
641 tions. Both the HadAM3 and the LMDZ4 sets of sea surface temperature
642 changes, and hence also precipitation source changes, agree with the broad
643 pattern of last interglacial sea surface temperature information (Fig. 10).
644 This means that neither set of simulation results can be definitely excluded
645 as unrepresentative of last interglacial changes. This is problematic, in that it
646 indicates that a very broad range of interglacial temperatures, across Green-
647 land, could be in agreement with a $> 3 \text{ ‰}$ increase in interglacial $\delta^{18}O$. In
648 essence anywhere between 4 and $>10 \text{ }^\circ\text{C}$ seems possible. Such a broad range
649 of uncertainty also affects the ability to be able to interpret past interglacial
650 changes in the elevation of the Greenland ice sheet: if significant sea sur-
651 face warming took place around the northern edge of Greenland, simulation
652 results imply that a reduced interglacial elevation of the central Greenland
653 ice sheet surface may not be necessary to explain the isotopically enriched
654 interglacial values. However, if this warming did not occur, larger eleva-
655 tion changes become more likely. Further isotopic modelling studies, which
656 also examine the impact of ice sheet, vegetation, and insolation driven $\delta^{18}O$
657 impacts, would be of considerable value in addressing this question.

658 In conclusion, this study represents an original contribution to the debate
659 regarding the drivers of isotope-temperature relationships. We have shown,
660 for the first time, that if seas to the north of Greenland warm by around
661 $+4$ to $+6 \text{ }^\circ\text{C}$, and sea ice is reduced, then central Greenland $\delta^{18}O$ rises of
662 $> 3 \text{ ‰}$ can be simulated at temperatures of $+5^\circ\text{C}$. Additional marine core
663 observations from northern Greenland, which help establish the magnitude
664 of interglacial changes in sea surface conditions, alongside further modelling
665 studies, will help in assessing whether a sea ice reduction is indeed the most
666 likely cause of high interglacial $\delta^{18}O$ in Greenland ice cores.

667 **Acknowledgements**

668 This is Past4Future contribution no 22. The research leading to these
669 results has received funding from the European Union’s Seventh Framework
670 programme (FP7/2007-2013) under grant agreement no 243908, the Agence
671 Nationale de la Recherche NEEM and GREENLAND projects, and UK-
672 NERC grant NE/J004804/1. It forms a part of the British Antarctic Survey
673 Polar Science for Planet Earth Programme. The LMDZ4 simulations were
674 run on the NEC-SX6 of the IDRIS computer center.

675 **References**

- 676 Adler, R.E., Polyak, L., Ortiz, J.D., Kaufman, D.S., Channell, J.E.T., Xuan,
677 C., Grottoli, A.G., Selln, E., Crawford, K.A., 2009. Sediment record from
678 the western Arctic Ocean with an improved Late Quaternary age reso-
679 lution: HOTRAX core HLY0503-8JPC, Mendeleev Ridge. *Global and*
680 *Planetary Change* 68, 18–29.
- 681 van de Berg, W.J., van den Broeke, M., Ettema, J., van Meijgaard, E.,
682 Kaspar, F., 2011. Significant contribution of insolation to Eemian melting
683 of the Greenland ice sheet. *Nature Geoscience* 4, 679–683.
- 684 Burgess, E.W., Forster, R.R., Box, J.E., Mosley-Thompson, E., Bromwich,
685 D.H., Bales, R.C., Smith, L.C., 2010. A spatially calibrated model of
686 annual accumulation rate on the Greenland Ice Sheet (19582007). *Journal*
687 *of Geophysical Research* 115, F02004+.
- 688 Burkhart, J.F., Hutterli, M., Bales, R.C., McConnell, J.R., 2004. Seasonal
689 accumulation timing and preservation of nitrate in firn at Summit, Green-
690 land. *Journal of Geophysical Research* 109, D19302+.
- 691 CAPE Project Members, 2006. Last Interglacial Arctic warmth confirms
692 polar amplification of climate change. *Quaternary Science Reviews* 25,
693 1383 – 1400.
- 694 Capron, E., Landais, A., Chappellaz, J., Schilt, A., Buiron, D., Dahl-Jensen,
695 D., Johnsen, S.J., Jouzel, J., Lemieux-Dudon, B., Loulergue, L., Leuen-
696 berger, M., Masson-Delmotte, V., Meyer, H., Oerter, H., Stenni, B., 2010.
697 Millennial and sub-millennial scale climatic variations recorded in polar ice
698 cores over the last glacial period. *Climate of the Past* 6, 345–365.

- 699 Chen, J.L., Wilson, C.R., Tapley, B.D., 2006. Satellite Gravity Measurements
700 Confirm Accelerated Melting of Greenland Ice Sheet. *Science* 313, 1958–
701 1960.
- 702 Colville, E.J., Carlson, A.E., Beard, B.L., Hatfield, R.G., Stoner, J.S., Reyes,
703 A.V., Ullman, D.J., 2011. Sr-Nd-pb isotope evidence for Ice-Sheet presence
704 on southern greenland during the last interglacial. *Science* 333, 620–623.
- 705 Cronin, T., Gemery, L., Jr., W.B., Jakobsson, M., Polyak, L., Brouwers],
706 E., 2010. Quaternary Sea-ice history in the Arctic Ocean based on a new
707 Ostracode sea-ice proxy. *Quaternary Science Reviews* 29, 3415 – 3429.
708 APEX: Arctic Palaeoclimate and its Extremes.
- 709 Cuffey, K., Clow, G., Alley, R., Stuiver, M., Waddington, E., Saltus, R.,
710 1995. Large Arctic temperature change at the Wisconsin-Holocene glacial
711 transition. *Science* 270, 455–458.
- 712 Cuffey, K., Paterson, W., 2010. *The Physics of Glaciers*, 4th Edition. Elsevier
713 Academic Press.
- 714 Cuffey, K.M., Marshall, S.J., 2000. Substantial contribution to sea-level rise
715 during the last interglacial from the Greenland ice sheet. *Nature* 404,
716 591–594.
- 717 Dahl-Jensen, D., Mosegaard, K., Gundestrup, N., Clow, G.D., Johnsen, S.J.,
718 Hansen, A.W., Balling, N., 1998. Past Temperatures Directly from the
719 Greenland Ice Sheet. *Science* 282, 268–271.
- 720 Dansgaard, W., 1964. Stable isotopes in precipitation. *Tellus* 16, 436–468.
- 721 Gordon, C., Cooper, C., Senior, C.A., Banks, H., Gregory, J.M., Johns, T.C.,
722 Mitchell, J.F.B., Wood, R.A., 2000. The simulation of SST, sea ice extents
723 and ocean heat transports in a version of the Hadley Centre coupled model
724 without flux adjustments. *Climate Dynamics* 16, 147–168.
- 725 Govin, A., Braconnot, P., Capron, E., Cortijo, E., Duplessy, J.C., Jansen,
726 E., Labeyrie, L., Landais, A., Marti, O., Michel, E., Mosquet, E., Rise-
727 brobakken, B., Swingedouw, D., Waelbroeck, C., 2012. Persistent influence
728 of ice sheet melting on high northern latitude climate during the early Last
729 Interglacial. *Climate of the Past* 8, 483–507.

- 730 GRIP Project Members, 1993. Climate instability during the last interglacial
731 period recorded in the GRIP ice core. *Nature* 364, 203–207.
- 732 Helsen, M., van de Wal, R., van den Broeke, M., 2007. The isotopic composi-
733 tion of present-day Antarctic snow in a Lagrangian atmospheric simulation.
734 *Journal of Climate* 20, 739–756.
- 735 Hoffmann, G., Heimann, M., 1997. Water isotope modeling in the Asian
736 monsoon region. *Quaternary International* 37, 115–128.
- 737 Hoffmann, G. Werner, M., Heimann, M., 1998. The Water Isotope Module of
738 the ECHAM Atmospheric General Circulation Model - A study on Time
739 Scales from Days to Several Years. *Journal of Geophysical Research* 103,
740 16871–16896.
- 741 Johnsen, S.J., Clausen, H.B., Cuffey, K.M., Schwander, J., Creyts, T., 2000.
742 Physics of Ice Core Records. Hokkaido University Press, Sapporo. volume
743 159. chapter Diffusion of stable isotopes in polar firn and ice: the isotope
744 effect in firn diffusion. pp. 121–140.
- 745 Johnsen, S.J., Dahl-Jensen, D., Dansgaard, W., Gundestrup, N., 1995.
746 Greenland palaeotemperatures derived from GRIP bore hole temperature
747 and ice core isotope profiles. *Tellus B* 47, 624–629.
- 748 Johnsen, S.J., Dahl-Jensen, D., Gundestrup, N., Steffensen, J.P., Clausen,
749 H.B., Miller, H., Masson-Delmotte, V., Sveinbjrnsdottir, A.E., White, J.,
750 2001. Oxygen isotope and palaeotemperature records from six Green-
751 land ice-core stations: Camp Century, Dye-3, GRIP, GISP2, Renland and
752 NorthGRIP. *Journal of Quaternary Science* 16, 299–307.
- 753 Johnsen, S.J., Dansgaard, W., Clausen, H.B., Langway, C.C., 1972. Oxygen
754 Isotope Profiles through the Antarctic and Greenland Ice Sheets. *Nature*
755 235, 429–434.
- 756 Jouzel, J., Alley, R.B., Cuffey, K.M., Dansgaard, W., Grootes, P., Hoffmann,
757 G., Johnsen, S.J., Koster, R.D., Peel, D., Shuman, C., Stievenard, M.,
758 Stuiver, M., White, J., 1997. Validity of the temperature reconstruction
759 from water isotopes in ice cores. *Journal of Geophysical Research - Oceans*
760 102, 26471–26487. 97JC01283.

- 761 Jouzel, J., Koster, R.D., Suozzo, R.J., Russell, G.L., 1994. Stable water
762 isotope behavior during the last glacial maximum: A general circulation
763 model analysis. *Journal of Geophysical Research* 99, 25791–25802.
- 764 Kobashi, T., Kawamura, K., Severinghaus, J.P., Barnola, J.M., Nakaegawa,
765 T., Vinther, B.M., Johnsen, S.J., Box, J.E., 2011. High variability of
766 Greenland surface temperature over the past 4000 years estimated from
767 trapped air in an ice core. *Geophysical Research Letters* 38, L21501.
- 768 Krinner, G., Genthon, C., Jouzel, J., 1997. GCM analysis of local influences
769 on ice core δ signals. *Geophysical Research Letters* 24, 2825–2828.
- 770 Krinner, G., Guicherd, B., Ox, K., Genthon, C., Magand, O., 2008. Influence
771 of oceanic boundary conditions in simulations of Antarctic climate and
772 surface mass balance change during the coming century. *Journal of Climate*
773 21, 938–962.
- 774 Krinner, G., Werner, M., 2003. Impact of precipitation seasonality changes
775 on isotopic signals in polar ice cores: a multi-model analysis. *Earth and*
776 *Planetary Science Letters* 4, 525–538.
- 777 Lachlan-Cope, T.A., Connolley, W.M., Turner, J., 2007. Effects of
778 tropical sea surface temperature (SST) errors on the Antarctic at-
779 mospheric circulation of HadCM3. *Geophysical Research Letters* 34.
780 Doi:10.1029/2006GL029067.
- 781 Landais, A., Chappellaz, J., Delmotte, M., Jouzel, J., Blunier, T., Bourg,
782 C., Caillon, N., Cherrier, S., Malaizé, B., Masson-Delmotte, V., Raynaud,
783 D., Schwander, J., Steffensen, J.P., 2003. A tentative reconstruction of
784 the last interglacial and glacial inception in Greenland based on new gas
785 measurements in the Greenland Ice Core Project (GRIP) ice core. *Journal*
786 *of Geophysical Research* 108, 4563+.
- 787 Landais, A., Masson-Delmotte, V., Jouzel, J., Raynaud, D., Johnsen, S., Hu-
788 ber, C., Leuenberger, M., Schwander, J., Minster, B., 2005. The glacial
789 inception as recorded in the NorthGRIP Greenland ice core: timing, struc-
790 ture and associated abrupt temperature changes. *Climate Dynamics* 26,
791 273–284.

- 792 Lang, N., Wolff, E.W., 2010. Interglacial and glacial variability from the
793 last 800 ka in marine, ice and terrestrial archives. *Climate of the Past*
794 *Discussions* 6, 2223–2266.
- 795 Langway, C., Oeschger, H., Dansgaard, W. (Eds.), 1985. Greenland ice core:
796 Geophysics, geochemistry and environment. volume Geophysical Mono-
797 graphs. American Geophysics Union, Washington D.C.
- 798 Leduc, G., Schneider, R., Kim, J.H., Lohmann, G., 2010. Holocene and
799 Eemian sea surface temperature trends as revealed by alkenone and Mg/Ca
800 paleothermometry. *Quaternary Science Reviews* 29, 989 – 1004.
- 801 Letreguilly, A., Reeh, N., Huybrechts, P., 1991. The Greenland ice sheet
802 through the last glacial-interglacial cycle. *Global and Planetary Change*
803 4, 385–394.
- 804 MARGO Project Members, 2009. Constraints on the magnitude and patterns
805 of ocean cooling at the last glacial maximum. *Nature Geoscience* 2, 127–
806 132.
- 807 Masson-Delmotte, V., Braconnot, P., Hoffmann, G., Jouzel, J., Kageyama,
808 M., Landais, A., Lejeune, Q., Risi, C., Sime, L., Sjolte, J., Swingedouw,
809 D., Vinther, B., 2011. Sensitivity of interglacial Greenland temperature
810 and $\delta^{18}\text{O}$ to orbital and CO_2 forcing: climate simulations and ice core data.
811 *Climate of the Past Discussions* 7, 1585–1630.
- 812 Masson-Delmotte, V., Buiron, D., Ekaykin, A., Frezzotti, M., Gallée, H.,
813 Jouzel, J., Krinner, G., Landais, A., Motoyama, H., Oerter, H., Pol, K.,
814 Pollard, D., Ritz, C., Schlosser, E., Sime, L.C., Sodemann, H., Stenni,
815 B., Uemura, R., Vimeux, F., 2010. A comparison of the present and
816 last interglacial periods in six Antarctic ice cores. *Climate of the Past*
817 *Discussions* 6, 2267–2333.
- 818 Masson-Delmotte, V., Dreyfus, G., Braconnot, P., Johnsen, S., Jouzel, J.,
819 Kageyama, M., Landais, A., Loutre, M.F., Nouet, J., Parrenin, F., Ray-
820 naud, D., Stenni, B., Tuenter, E., 2006. Past temperature reconstructions
821 from deep ice cores: relevance for future climate change. *Climate of the*
822 *Past* 2, 145–165.
- 823 Masson-Delmotte, V., Jouzel, J., Landais, A., Stievenard, M., Johnsen, S.J.,
824 White, J.W.C., Werner, M., Sveinbjornsdottir, A., Fuhrer, K., 2005. GRIP

- 825 Deuterium Excess Reveals Rapid and Orbital-Scale Changes in Greenland
826 Moisture Origin. *Science* 309, 118–121.
- 827 NGRIP Project Members, 2004. High-Resolution record of northern hemi-
828 sphere climate extending into the last interglacial period. *Nature* 431,
829 147–151.
- 830 Noone, D., 2008. The influence of midlatitude and tropical overturning circu-
831 lation on the isotopic composition of atmospheric water vapor and Antarc-
832 tic precipitation. *Journal of Geophysical Research* 113, D04102+.
- 833 Noone, D., Simmonds, I., 2004. Sea ice control of water isotope transport
834 to Antarctica and implications for ice core interpretation. *Journal of Geo-
835 physical Research - Atmospheres* 109, D07105+.
- 836 Noone, D., Sturm, C., 2010. Isoscapes: Understanding movement, patterns,
837 and process on Earth through isotope mapping. Springer. chapter Com-
838 prehensive dynamical models of global and regional water isotope distri-
839 butions. p. 487.
- 840 Nørgaard-Pedersen, N., Mikkelsen, N., Lassen, S.J., Kristoffersen, Y., Shel-
841 don, E., 2007. Reduced sea ice concentrations in the Arctic Ocean during
842 the last interglacial period revealed by sediment cores off northern Green-
843 land. *Paleoceanography* 22, PA1218+.
- 844 Otto-Bliesner, B.L., Marshall, S.J., Overpeck, J.T., Miller, G.H., Hu, A.,
845 members, C.L.I.P., 2006. Simulating Arctic Climate Warmth and Icefield
846 Retreat in the Last Interglaciation. *Science* 311, 1751–1753.
- 847 Pope, V.D., Gallani, M.L., Rowntree, P.R., Stratton, R.A., 2000. The im-
848 pact of new physical parametrizations in the Hadley Centre climate model:
849 HadAM3. *Climate Dynamics* 16, 123–146.
- 850 Rayner, N.A., Parker, D.E., Horton, E.B., Folland, C.K., Alexander, L.V.,
851 Rowell, D.P., Kent, E.C., Kaplan, A., 2003. Global analyses of sea sur-
852 face temperature, sea ice, and night marine air temperature since the late
853 nineteenth century. *Journal of Geophysical Research* 108, 4407+.
- 854 Risi, C., Bony, S., Vimeux, F., Jouzel, J., 2010. Water-stable isotopes in
855 the LMDZ4 general circulation model: Model evaluation for present-day

- 856 and past climates and applications to climatic interpretations of tropical
857 isotopic records. *Journal of Geophysical Research* 115, D12118.
- 858 Schmidt, G.A., LeGrande, A.N., Hoffmann, G., 2007. Water isotope ex-
859 pressions of intrinsic and forced variability in a coupled ocean-atmosphere
860 model. *Journal of Geophysical Research* D10103, –.
- 861 Schurgers, G., Mikolajewicz, U., Gröger, M., Maier-Reimer, E., Vizcaíno, M.,
862 Winguth, A., 2007. The effect of land surface changes on eemian climate.
863 *Climate Dynamics* 29, 357–373.
- 864 Severinghaus, J.P., Brook, E.J., 1999. Abrupt climate change at the end of
865 the last glacial period inferred from trapped air in polar ice. *Science* 286,
866 930–934.
- 867 Severinghaus, J.P., Sowers, T., Brook, E.J., Alley, R.B., Bender, M.L., 1998.
868 Timing of abrupt climate change at the end of the Younger Dryas interval
869 from thermally fractionated gases in polar ice. *Nature* 391, 141–146.
- 870 Sime, L.C., Lang, N., Thomas, E.R., Mulvaney, R., 2011. On high resolution
871 sampling of short ice cores: Dating and temperature information recovery
872 from Antarctic Peninsula virtual cores. *Journal of Geophysical Research -*
873 *Atmospheres* 116, D20117.
- 874 Sime, L.C., Marshall, G.J., Mulvaney, R., Thomas, E.R., 2009a. Interpret-
875 ing temperature information from ice cores along the Antarctic Peninsula:
876 ERA40 analysis. *Geophysical Research Letters* 36, L18801.
- 877 Sime, L.C., Stevens, D.P., Heywood, K.J., Oliver, K.I.C., 2006. A De-
878 composition of the Atlantic Meridional Overturning. *Journal of Physical*
879 *Oceanography* 36, 2253–2270.
- 880 Sime, L.C., Tindall, J., Wolff, E., Connolley, W., Valdes, P., 2008.
881 The Antarctic isotopic thermometer during a CO₂ forced warming
882 event. *Journal of Geophysical Research - Atmospheres* D24119. Doi:
883 10.1029/2008JD010395.
- 884 Sime, L.C., Wolff, E.W., Oliver, K.I.C., Tindall, J.C., 2009b. Evidence for
885 warmer interglacials in East Antarctic ice cores. *Nature* 462, 342–345.

- 886 Sjolte, J., Hoffmann, G., Johnsen, S.J., Vinther, B.M., Masson-Delmotte, V.,
887 Sturm, C., 2011. Modeling the water isotopes in Greenland precipitation
888 19592001 with the meso-scale model REMO-iso. *Journal of Geophysical*
889 *Research* 116, D18105.
- 890 Stroeve, J., Holland, M.M., Meier, W., Scambos, T., Serreze, M., 2007. Arctic
891 sea ice decline: Faster than forecast. *Geophysical Research Letters* 34,
892 L09501+.
- 893 Suwa, M., von Fischer, J.C., Bender, M.L., Landais, A., Brook, E.J., 2006.
894 Chronology reconstruction for the disturbed bottom section of the GISP2
895 and the GRIP ice cores: Implications for termination II in greenland.
896 *Journal of Geophysical Research* 111, D02101+.
- 897 Svensson, A., Andersen, K.K., Bigler, M., Clausen, H.B., Dahl-Jensen, D.,
898 Davies, S.M., Johnsen, S.J., Muscheler, R., Parrenin, F., Rasmussen, S.O.,
899 Röthlisberger, R., Seierstad, I., Steffensen, J.P., Vinther, B.M., 2008. A
900 60 000 year Greenland stratigraphic ice core chronology. *Climate of the*
901 *Past* 4, 47–57.
- 902 Tindall, J.C., Valdes, P.J., Sime, L.C., 2009. Stable water isotopes in
903 HadCM3: Isotopic signature of El Niño Southern Oscillation and the tropi-
904 cal amount effect. *Journal of Geophysical Research* 114, D04111.
- 905 Turney, C.S., Jones, R.T., 2010. Does the Agulhas Current amplify global
906 temperatures during super-interglacials? *Journal of Quaternary Science*
907 25, 839–843.
- 908 Velicogna, I., 2009. Increasing rates of ice mass loss from the Greenland and
909 Antarctic ice sheets revealed by GRACE. *Geophysical Research Letters*
910 36, L19503.
- 911 Vinther, B., Jones, P., Briffa, K., Clausen, H., Andersen, K., Dahl-Jensen,
912 D., Johnsen, S., 2010. Climatic signals in multiple highly resolved stable
913 isotope records from Greenland. *Quaternary Science Reviews* 29, 522 –
914 538.
- 915 Vinther, B.M., Buchardt, S.L., Clausen, H.B., Dahl-Jensen, D., Johnsen,
916 S.J., Fisher, D.A., Koerner, R.M., Raynaud, D., Lipenkov, V., Andersen,
917 K.K., Blunier, T., Rasmussen, S.O., Steffensen, J.P., Svensson, A.M., 2009.
918 Holocene thinning of the Greenland ice sheet. *Nature* 461, 385–388.

- 919 Watson, A.J., Naveira Garabato, A.C., 2006. The role of southern ocean
920 mixing and upwelling in glacial-interglacial atmospheric co2 change. *Tellus*
921 *Series B Chemical And Physical Meteorology* 58, 73–87.
- 922 Werner, M., Heimann, M., 2002. Modeling interannual variability of water
923 isotopes in Greenland and Antarctica. *Journal of Geophysical Research D*
924 *- Atmospheres* 107.
- 925 Werner, M., Langebroek, P.M., Carlsen, T., Herold, M., Lohmann, G., 2011.
926 Stable water isotopes in the ECHAM5 general circulation model: Toward
927 high-resolution isotope modeling on a global scale. *Journal of Geophysical*
928 *Research* 116, D15109+.
- 929 Werner, M., Mikolajewicz, U., Heimann, M., Hoffmann, G., 2000. Bore-
930 hole versus isotope temperatures on Greenland: Seasonality does matter.
931 *Geophysical Research Letters* 27, 723–726.
- 932 Wunsch, C., 2003. Determining paleoceanographic circulations, with empha-
933 sis on the last glacial maximum. *Quaternary Science Reviews* 22, 371 –
934 385.

Table 1: Simulation sea surface condition (SSC) and atmospheric gas boundary conditions. Simulations are run for 20 or more years.

Experiment	Applied SSC anomaly		HadCM3 and IPSL atmosphere		
	SST	Sea ice	CO_2 <i>ppmv</i> ^a	N_2O <i>ppbv</i> ^b	CH_4 <i>ppmv</i>
Present day HadAM3 ^c	HadISST	HadISST	353	310	1.72
Present day LMDZ4 ^d	AMIP ^e	AMIP	348	306	1.65
Warm HadAM3 (SRES A1B)	HadCM3	HadCM3	720	370	2.0
Very warm HadAM3 (SRES A2)	HadCM3	HadCM3	820	370	2.0
Warm LMDZ4 (CO2 x 2)	IPSL	IPSL	696	306	1.65
Very warm LMDZ4 (CO2 x 4)	IPSL	IPSL	1392	306	1.65
SST HadAM3 (SRES A1B)	HadCM3	HadISST	720	370	2.0
SeaIce HadAM3 (SRES A1B)	HadISST	HadCM3	720	370	2.0

^a *ppmv* - parts per million by volume. ^b *ppbv* - parts per billion by volume. ^c Present-day centered on 1990.

^d Present-day centered on 1992. ^e Atmospheric Model Intercomparison Project. See text for further details.

Table 2: Compilation of observations of Northern Hemisphere sea ice change for warmer interglacial conditions.

Site Name	Latitude °N [deg.min]	Longitude °W [deg.min]	Water depth [m]	Time MIS or ky	Proxy	Evaluation
GreenICE (c11)	84.49	74.16	1089	MIS5e-present (approx 128-0 ky)	Subpolar forams	Reduced sea ice in MIS 5a compared to present suggestion about season Pattern similar to Holo indicator missing in ear (peak) interglacial, and at moderate levels later
NP26-5/32	78.59	178.09	1435	130-0 ky	Ostracodes	Pattern similar to Holo (peak) interglacial, and at moderate levels later
Oden96/12-1pc	87.05	144.46	1003	240-0 ky	Ostracodes	Pattern similar to Holo indicator missing in ear (peak) interglacial, and at moderate levels later
PS2200-5	85.19	14.00	1073	240-0 ky	Ostracodes	Pattern similar to Holo indicator missing in ear (peak) interglacial, and at moderate levels later
PS1243	69.23	6.32	2710	240-0 ky	Ostracodes	Indicator absent in 5E
M23214	53.32	20.17	2119	196-0 ky	Ostracodes	Indicator absent in 5E
HLY0503-8JPC	79.36	172.30	2792	MIS7-1 (approx 250-0 ky)	Subpolar forams	Reduced sea ice in MIS 5a compared to present Suggests seasonally ice-

Table 3: Annual mean present day (and warmer climate) simulation results (and anomalies) for central Greenland (> 1300 m). Temperature, precipitation, $\delta^{18}O$, and temporal $\delta^{18}O$ against temperature gradients, as specified.

Experiment	Temperature $^{\circ}C$	Precipitation $kg\ m^2\ yr^{-1}$ (%)	$\delta^{18}O$ ‰	gradient ‰ per $^{\circ}C$
Present day simulation results				
HadAM3 present day	-24.0	325.8	-23.9	
LMDZ4 present day	-18.8	454.0	-28.3	
Warmer simulation anomalies				
HadAM3 SRES A1B	+4.7	+92.8 (+28.5)	+3.6	0.76
HadAM3 SRES A2	+5.4	+117.1 (+35.9)	+3.9	0.71
LMDZ4 CO2 x 2	+3.3	+74.1 (+16.4)	+0.31	0.09
LMDZ4 CO2 x 4	+7.3	+176.1 (+38.8)	+1.79	0.25
HadAM3 SRES A1B SST	+3.4	+57.9 (+17.8)	+2.1	0.63
HadAM3 SRES A1B SeaIce	+0.84	+21.5 (+6.6)	+0.25	0.29

Table 4: The percentage of simulated present day central Greenland precipitation which is sourced from different regions, and the mean $\delta^{18}O$ precipitation value associated with each source region.

Precipitation source region	HadAM3 precipitation (%)	LMDZ4 precipitation (%)	HadAM3 $\delta^{18}O$ in precipitation (‰)	LMDZ4 $\delta^{18}O$ in precipitation (‰)
High latitude	18	20	+5.1	+2.0
Mid-low latitude	51	51	-37.1	-38.2
Continental	31	29	-29.6	-29.2

Figure 1: Ice cores across Greenland which may feature some last interglacial ice, and maximum difference between present day (0-3 ky) and maximum ‘last interglacial’ values. Map (a) shows the sites of the ice cores, where possible $\delta^{18}O$ last interglacial records are available. Numbers next to the core sites indicate the difference between the present day (0 - 3 ky) $\delta^{18}O$ and the maximum (before 100 ky) ice core $\delta^{18}O$ values. The present day to ‘maximum $\delta^{18}O$ values’ given on map (a) have question marks or > marks to indicate the available values are questionable or likely underestimates of true peak last interglacial differences. For visual simplicity, we have placed the isotopically lightest near bed Renland ice ($\delta^{18}O$ value of about -24 ‰, true age not known) at 123 ky (circled). It is likely that this also does not represent peak interglacial values.

Figure 2: Comparison between HadAM3 present day simulated and observed (see Appendix B) Greenland values. Shading shows the mean simulation (20 year average) (a) surface temperature ($^{\circ}C$), (b) precipitation ($kg\ m^{-2}\ yr^{-1}$), (c) $\delta^{18}O$ (‰), (d) δD (‰), (e) deuterium excess (anomalies relative to Greenland average), and (f) orography (m). The square symbols on each panel give equivalent observed values as detailed in Table 2. For easy of comparison simulation results are presented after linear interpolation onto a $50\ km \times 50\ km$ equal area grid (Sime et al., 2008).

Figure 3: As Fig. 2 but for LMDZ4 present day simulation. Shading shows (a) surface temperature ($^{\circ}C$), (b) precipitation ($kg\ m^{-2}\ yr^{-1}$), (c) $\delta^{18}O$ (‰), (d) δD (‰), (e) deuterium excess (anomalies relative to Greenland average), and (f) orography (m). The square symbols on each panels give equivalent observed values as detailed in Table B.2.

Figure 4: Differences between the present day and warmer simulation climatic and isotopic results. (a,b) HadAM3 SRES A1B simulation; (c,d) HadAM3 SRES A2 simulation; (e,f) LMDZ4 CO2 x 2; and (g,h) LMDZ4 CO2 x 4. Left hand panels (a,c,e,g) shading (and contouring) over Greenland shows the difference between the present day and individual simulation values of $\delta^{18}O$ (and surface temperature) values, shading over the ocean areas shows anomalous sea ice concentrations. Right hand panel (b,d,f,h) shading (and contouring) over Greenland shows the difference between the present day and individual sensitivity simulation values of d-excess (and precipitation changes, in percentage) values, shading over the ocean areas shows anomalous sea surface temperatures. In each case, the shading over the ocean areas show the forcing applied to the atmospheric model, whilst over Greenland the shading (and contouring) shows the model response to the boundary condition changes.

Figure 5: Changes in central Greenland seasonality between the HadAM3 SRES A1B and present day simulation, and the LMDZ4 CO2 x 4 and present day simulation. Panel (a) shows the HadAM3 model response over Greenland for mean monthly central Greenland ($> 1300\ m$) anomalous temperature (K), $\delta^{18}O$ (‰), precipitation ($kg\ m^{-2}\ yr^{-1}$), and d-excess. Panel (b) shows results for LMDZ4.

Figure 6: Changes in ocean and sea ice surface seasonality between the HadAM3 SRES A1B and present day simulation, and the LMDZ4 CO₂ × 4 and present day simulation. Panel (a) shows HadAM3 changes in: Atlantic north of 70°N sea surface temperature (solid line); North Atlantic north of 45°N sea surface temperature changes (dashed line); North Atlantic sea ice area changes (solid line); Northern Hemisphere sea ice area changes (dashed line); Atlantic all north of 70°N evaporation changes (solid line); North Atlantic all north of 45°N evaporation changes (dashed line). Panel (b) shows similar changes for the LMDZ4 results. All solid (dashed) results are on the left (right) axis.

Figure 7: HadAM3 sensitivity simulation results. (a,b) HadAM3 SRES A1B SST simulation; (c,d) HadAM3 SRES A1B SeaIce simulation; (e,f) effects of SST and SeaIce simulation results added together. Left hand panels (a,c,e) shading (and contouring) over Greenland shows the difference between the present day and individual simulation values of $\delta^{18}O$ ‰ (and surface temperature °C) values, shading over the ocean areas shows anomalous ice concentrations. Right hand panel (b,d,f) shading (and contouring) over Greenland shows the difference between the present day and individual sensitivity simulation values of d-excess (and precipitation changes, in percentage) values, shading over the ocean areas shows anomalous sea surface temperatures.

Figure 8: Changes in the amount of precipitation sourced from high-latitude (local) regions between the present day and individual simulation results: (a) HadAM3 SRES A1B and (b) LMDZ4 CO₂ × 4. Note that any reduction in the high-latitude sourced percentage means that an equivalent rise in the proportion of mid-low latitude and continentally sourced precipitation vapour is required to balance the budget.

Figure 9: Shading shows the $\delta^{18}O$ against temperature gradient (‰ per °C) between the present day and individual simulation results. (a) HadAM3 SRES A1B; (b) HadAM3 SRES A2; (c) LMDZ4 CO₂ × 2; (d) LMDZ4 CO₂ × 4; (e) HadAM3 SRES A1B SST; and (f) HadAM3 SRES A1B SeaIce. The contouring for the HadAM3 results shows the temperature biasing (K) changes (cannot be calculated for LMDZ4 results because necessary variables not available).

Figure 10: Observations of last interglacial sea surface temperature (K) and sea ice anomalies plotted over the top of (a) HadAM3 SRES A1B and (b) LMDZ4 CO₂ × 4 sea surface temperature changes (K).

935 **Appendix A. Further details on the isotopic simulations:**

936 The HadAM3 present day boundary conditions are based on a monthly
937 average of 1980-1999 HadISST sea surface temperature and sea-ice data
938 (Rayner et al., 2003; Sime et al., 2008). The level of atmospheric CO₂ for the
939 present day run is 353 ppmv. The LMDZ4 present day run uses very similar
940 standards, using a monthly average of the sea surface condition observational
941 record from 1978-2007, and a level of atmospheric CO₂ of 348 ppm.

942 The approach used to generate the warmer than present day simula-
943 tions in the two AGCMs is very similar. Coupled ocean-atmosphere versions
944 (HadCM3 and IPSL), of the respective AGCM are used to simulate warmer
945 than present day climates. The sea surface temperature anomalies from each
946 coupled model simulation are then applied to the present day simulation
947 (Sime et al., 2008; Masson-Delmotte et al., 2011). The use of anomalies re-
948 duces the impact of known model errors. Both the HadCM3 and the IPSL
949 model sea surface temperature outputs have regional biases compared with
950 the observed present day sea surface temperature (Lachlan-Cope et al., 2007).
951 These biases can affect the modelled climatology. However, by applying the
952 HadCM3 and IPSL sea surface temperature fields as anomalies to the present
953 day sea surface temperature boundary conditions, the effect of these biases is
954 minimised (*e.g.* Krinner et al., 2008). Please see also Sime et al. (2008), Risi
955 et al. (2010), and Masson-Delmotte et al. (2011) for additional background
956 details.

957 For the HadAM3 warmer simulations the sea surface condition anoma-
958 lies are obtained from the HadCM3 World Climate Research Programme's
959 Coupled Model Inter-comparison Project phase 3 simulations. These sim-
960 ulations use the ocean-atmosphere coupled HadCM3 model (Gordon et al.,
961 2000; Sime et al., 2006). The CO₂ and other atmospheric composition is
962 based on Special Report on Emissions Scenarios (SRES) A1B and A2 ex-
963 periments (see Table 1 for values), in each case focussed on the year 2100.
964 The LMDZ4 warmer than present day simulations used here are very simi-
965 lar to to the HadAM3 simulations. The boundary conditions are also based
966 on GHG driven (Table 1) IPSL simulation sea surface condition anomalies
967 (Masson-Delmotte et al., 2011). Two additional isotopic HadAM3 sensitivity
968 experiments individually simulate the effect of the SRES A1B warmer sea
969 surface temperatures (SST) and the SRES A1B sea ice changes (SeaIce). All
970 simulations use fixed (present day) Greenland ice sheet elevations. Please
971 see Table 1 for a summary of the simulations.

972 **Appendix B. Evaluation of the present day model simulations against**
973 **observations:**

974 *Appendix B.1. Mean annual results:*

975 Present day observations from the surface of the Greenland ice sheet
976 were provided by Vinther et al. (2010) and Sjolte et al. (2011). Table B.3
977 provides a mean of these Table B.2 observations and the equivalent mean
978 simulation values, using co-located model results. See also main text Ta-
979 ble 3 and summary results, for the alternative simulation results using the
980 Masson-Delmotte et al. (2011) definition of central Greenland *i.e.* using all
981 points higher than 1300 m. The available observations (Table B.2) suggest
982 that the HadAM3 present day simulation temperature is on average, 1.9°C
983 warmer than the available observational values. For LMDZ4, the average
984 temperature is 9.1°C too warm. Note, available observational sites are not
985 equally representative of the whole of central Greenland. Whilst this unequal
986 representation effect is minimised by our comparison through co-location of
987 our model outputs, the comparison nevertheless is more representative of the
988 central cold region (see also Fig. 2a and 3a for the position of the available
989 observations).

990 The simulated annual mean precipitation values compare reasonably well
991 with the available accumulation observations. Note, as with temperature,
992 the observations are mainly representative of the highest, coldest, and driest
993 region. The HadAM3 simulation is 4.8 kg m⁻² yr⁻¹, or 26%, too dry com-
994 pared with these available observations, and the LMDZ4 simulation is 8.12
995 kg m⁻² yr⁻¹, or 44%, too wet. The wetter than observed LMDZ4 results are
996 likely related to the warmer than observed simulated temperatures. For both
997 HadAM3 and LMDZ4 the overall geographical pattern of the observations
998 and simulation results compare quite well (Fig. 2b and 3b) although com-
999 parison with additional observational evidence (*e.g.* Burgess et al., 2010)
1000 suggests that, in common with other models (Sjolte et al., 2011), simulated
1001 southern Greenland precipitation is likely too high.

1002 The annual mean isotopic values of the precipitation, in each simulation,
1003 are heavier than the observations (see also Fig. 2c and 3c). For HadAM3,
1004 comparison with the available observations suggests the HadAM3 simulation
1005 may on average be 8.6 ‰ too heavy, whilst LMDZ4 is closer to observations
1006 at 3.9 ‰ too heavy. The δD results follow a very similar pattern (see
1007 also Fig. 2d and 3d). This model-observation isotopic offset, particularly
1008 for HadAM3, seems too large to be simply explained by the warmer than

1009 observed model temperatures. The orographic representation of Greenland
1010 is reasonable accurate for central regions (Fig. 2f) and precipitation amount
1011 is generally reasonable, thus there seems no obvious reason in the mean
1012 annual results for the isotopic offset. Some similar heavy $\delta^{18}O$ biases also
1013 appear also be present in some other models (*e.g.* Hoffmann and Heimann,
1014 1998; Sjolte et al., 2011). For HadAM3, and perhaps also other models,
1015 one possibility to explain the model-observation different is that the seasonal
1016 representation of isotopes in precipitation is not accurate.

1017 *Appendix B.1.1. Seasonal results:*

1018 Danish Meteorological Institute (DMI) station observations (see Fig. B.11,
1019 for station positions) of monthly temperature provide a useful resource for
1020 checking monthly simulated temperatures. The monthly station observations
1021 are available over different observation periods. In some cases, the records
1022 are also split into more than one series: in these cases, the original series are
1023 treated as separate observational sets. Fig. B.12 shows the mean of each of
1024 these DMI observational records, with a standard deviation envelope (of \pm
1025 2 standard deviations to each side of the mean) in black and grey. Plotted
1026 over the top are results from the present HadAM3 (red) and LMDZ4 (blue)
1027 simulations, in each case co-located with the observed record.

1028 The results show that the seasonality of the temperature cycle in each
1029 model is generally reasonable, with the maximum and minimum monthly
1030 model-observation temperatures co-incident or within a month at the ma-
1031 jority of the sites. Most of the DMI observation sites are situated close to
1032 the coast, and are thus less useful for a more detailed evaluation the sim-
1033 ulation performance over the central Greenland region. However the latter
1034 panels show results from Summit and Dye 2/3 sites (Fig. B.12). These tend
1035 to suggest that the simulated seasonal cycle of temperature, over central
1036 Greenland, is too warm and the amplitude is too small in LMDZ4, whilst
1037 in HadAM3 the amplitude may be a little too large (as suggested in Section
1038 3.1). For the more coastal sites, there is more variety in the relationship
1039 between the observed and simulated results. This is at least partly due to
1040 the HadAM3 and LMDZ4 model resolution, which is too coarse to give a
1041 good representation of the complex coastline and topography.

1042 The seasonality of central Greenland precipitation for HadAM3 looks
1043 reasonable in comparison with the available observational records: both
1044 HadAM3 and the Burkhardt et al. (2004) observations for Greenland Summit
1045 also show a single August-September peak in accumulation. The LMDZ4

1046 precipitation seasonality is less uni-modal, which agrees less well with the
1047 Burkhart et al. (2004) precipitation seasonality observations.

1048 Fig. B.13 shows the present day precipitation and $\delta^{18}O$ seasonality for
1049 HadAM3, LMDZ4, and observational records (Sjolte et al., 2011). In each
1050 case, the top 20 years of each core was used to obtain the mean seasonal
1051 amplitude. Although similar model and observation methods were used for
1052 averaging the summer and winter values, the simulated HadAM3 summer
1053 $\delta^{18}O$ values seem to be 8.9 ‰ too enriched, whilst the winter values seem
1054 to be 5.6 ‰ too enriched compared with the observations. This affects
1055 the average annual offset (of 8.6 ‰ too heavy). The summer offset has
1056 a more dominant effect on the annual mean due to the larger amount of
1057 simulated HadAM3 summertime precipitation (Fig. B.13c). Additionally,
1058 the simulated 3.4 ‰ seasonal $\delta^{18}O$ amplitude is too large, as likely is the
1059 seasonal temperature amplitude. However, difficulties in accurately dating
1060 (*e.g.* Sime et al., 2011), and back diffusing the isotopic results, may reduce
1061 the amplitude of the core seasonal $\delta^{18}O$ amplitude, compared to its origi-
1062 nal amplitude (Johnsen et al., 2000; Vinther et al., 2010). This may partly
1063 explain the discrepancy between the simulated HadAM3 and observed ice
1064 core seasonal $\delta^{18}O$ amplitude. For LMDZ4, the summer $\delta^{18}O$ values are 2.2
1065 ‰ too enriched, whilst the winter values are 4.4 ‰ too enriched, compared
1066 with observations. This leads to an average annual offset which is 3.9 ‰ too
1067 heavy. Unlike HadAM3, LMDZ4 precipitation is less seasonal, so the offset
1068 is not strongly dominated by the summer precipitation. The simulated sea-
1069 sonal $\delta^{18}O$ amplitude for LMDZ4 is on average 2.2 ‰. In percentage terms,
1070 the LMDZ4 simulation of the $\delta^{18}O$ cycle amplitude is 41% of the observed
1071 amplitude, whereas the HadAM3 cycle is 190% of the observed amplitude.

Table B.5: Greenland observations of temperature, accumulation, $\delta^{18}O$. The observations were compiled by Vinther et al. (2010); Sjolte et al. (2011) and by Valerie Masson-Delmotte.

Longitude °W	Latitude °N	Temperature °C	Accumulation kg m ² yr ⁻¹	$\delta^{18}O$ ‰
37.65	73.03	-	14.10	-36.75
37.63	73.94	-	11.70	-37.08
37.63	74.85	-32.20	10.60	-37.4
36.40	75.72	-32.90	10.49	-36.66
36.40	76.62	-	11.40	-36.68
36.39	77.52	-31.00	11.83	-35.6
37.95	79.23	-	9.75	-34.9
41.14	80.00	-	10.22	-33.65
37.65	73.03	-	17.17	-36.49
37.65	73.50	-32.30	15.52	-38.18
37.63	73.94	-	13.75	-38.97
37.63	74.40	-32.70	13.32	-36.68
37.63	74.85	-32.20	12.64	-38.27
37.63	75.25	-	11.00	-36.93
37.21	75.25	-	14.11	-39.59
36.91	75.28	-	11.58	-36.19
36.39	75.50	-32.60	11.69	-36.42
39.54	75.57	-	11.66	-36.39
36.33	75.65	-	12.90	-37.23
36.40	75.72	-32.90	13.59	-36.87
36.40	76.17	-	13.12	-38.44
36.40	76.62	-	10.45	-34.94
37.37	76.62	-	11.47	-36.20
34.46	76.62	-	14.81	-36.02
36.40	77.07	-31.10	12.38	-36.83
36.39	77.52	-31.00	11.01	-35.02
36.40	78.00	-30.90	13.27	-34.7
36.44	78.42	-	11.50	-32.63
36.50	78.83	-	10.83	-34.86
37.95	79.23	-	9.75	-34.72
39.51	79.62	-	11.30	-35.51
41.14	80.00	-	12.01	-35.45
41.13	80.36	-	13.08	-32.64
37.63	73.94	-	12.28	-37.29
36.40	76.62	38	10.98	-37.04
41.14	80.00	-	10.40	-33.87
37.63	73.94	-	12.25	-37.32
36.40	76.62	-	10.40	-36.46
41.14	80.00	-	10.17	-34.47
37.63	73.94	-	14.20	-37.14
36.40	76.62	-	9.90	-36.67

Table B.2: Continued table.

Longitude °W	Latitude °N	Temperature °C	Accumulation kg m ² yr ⁻¹	$\delta^{18}O$ ‰
68.83	76.52	-11.60	-	-24.17
16.67	81.60	-17.28	-	-25.15
48.12	61.22	1.200	-	-11.98
18.40	76.46	-11.90	-	-18.54
22.00	70.50	-7.59	-	-13.78
43.07	60.08	0.73	-	-9.76
43.83	65.18	-	56.00	-27.40
44.50	70.30	-	54.00	-28.87
37.32	71.12	-	28.90	-34.18
35.82	70.63	-	29.20	-33.08
37.48	70.65	-	30.60	-33.50
39.62	70.64	-	35.40	-32.51
35.85	71.76	-	21.50	-35.61
35.84	71.15	-	24.90	-34.83
26.73	71.27	-	50.00	-27.23
37.64	72.58	-	23.00	-35.10

Table B.3: Observational and simulation averages. Mean of available Table B.2 observations (see Fig. 2 and B.13 for locations) and co-located simulation results.

Obs / Experiment	Temperature °C	Accumulation kg m ² yr ⁻¹	$\delta^{18}O$		
			annual ‰	summer ‰	winter ‰
Observations (Table B.2)	-32.0	18.3	-33.1	-29.4	-35.4
HadAM3 Present day	-30.0	21.6	-26.8	-20.4	-27.5
LMDZ4 Present day	-22.8	26.4	-27.5	-26.2	-31.5
HadAM3 SRES A1B	-24.4	30.7	-22.8	-18.3	-24.7
HadAM3 SRES A2	-23.5	33.5	-22.2	-18.2	-24.2
LMDZ4 CO2 x 2	-19.5	32.1	-28.4	-26.9	-30.5
LMDZ4 CO2 x 4	-15.1	41.2	-27.5	-26.2	-28.4
HadAM3 SRES A1B SST	-26.0	26.4	-24.2	-18.9	-26.0
HadAM3 SRES A1B SeaIce	-28.6	24.5	-26.6	-21.0	-27.0

Figure B.11: The location of DMI (Danish Meteorological Institute) observational sites.

Figure B.12: DMI monthly mean temperatures (black) and equivalent simulated HadAM3 (red) and LMDZ4 (blue) results. See Fig. B.11 for the location of the DMI observational stations. Grey envelope shows ± 2 standard deviations to each side of the observed mean. Length of records are shown in individual panel labels.

Figure B.13: The seasonality of the HadAM3 and LMDZ4 present day simulations. Panel (a) shows the HadAM3 summer minus winter simulation $\delta^{18}O$ (‰) seasonality (shaded) with similar core site seasonality observations (Vinther et al., 2010; Sjolte et al., 2011) overlain using shaded squares. Panel (b) shows similar results for the LMDZ4 present day simulation. Note that for clarity the colorbars are rescaled between the two simulations. (c) Lines show the mean monthly central Greenland (> 1300 m) values for the present day HadAM3 (solid lines) and LMDZ4 (dashed line) simulation of temperature, $\delta^{18}O$, precipitation, and d-excess.

1072 **Appendix C. Checking model dependence: Do the models HadAM3**
1073 **and LMDZ4 give similar results?**

1074 In order to check the sensitivity of results to the inter-model atmospheric
1075 physics, two original HadAM3 experiments are repeated using LMDZ4. Sea
1076 surface boundary conditions identical to the HadAM3 present day and HadAM3
1077 SRES A1B experiments (Table 1) are applied to LMDZ4: in each case, the
1078 LMDZ4 experiments are run using the HadAM3 boundary condition files.
1079 This is useful because it allows us to check for impacts of physical differences
1080 between the LMDZ4 and HadAM3 models. Computational restrictions mean
1081 that these additional experiments are run for three years.

1082 Comparing Fig. C.14a to Fig. 4a for LMDZ4 versus HadAM3, allows an
1083 inter-atmospheric model check of the temperature and $\delta^{18}O$ changes. The
1084 identical LMDZ4 and HadAM3 experiments show a similar pattern of warm-
1085 ing and $\delta^{18}O$ enrichment. This indicates that the sea surface temperature
1086 changes are the main driver of the Greenland climate and isotopic changes,
1087 rather than inter-model difference in atmospheric or isotopic physics. It also
1088 provides additional evidence that it is these sea surface condition changes
1089 (rather than any inter-model physics differences) which lead uncertainties
1090 in interpreting past Greenland $\delta^{18}O$ changes in terms of temperature shifts.
1091 This is confirmed by Fig. C.14b, which shows the $\delta^{18}O$ against tempera-
1092 ture gradient ($\text{‰ per } ^\circ\text{C}$) between the same additional LMDZ4 simulations.
1093 Like the HadAM3 equivalent Fig. 9a gradient results, much higher gradients
1094 across Greenland arise when LMDZ4 is forced by the larger HadCM3 A1B
1095 local sea surface warming to the north and east of Greenland. Additionally,
1096 the match between the contouring and shading on Fig. C.14b confirms that,
1097 like HadAM3, precipitation-temperature biasing changes drive most of the
1098 LMDZ4 smaller-scale geographical variability in the temporal $\delta^{18}O$ against
1099 temperature gradient.

Table C.4: Additional duplicate and water tagged simulations performed using LMDZ4

Isotopic model	Experiment	Applied SSC anomaly		CO_2 [ppmv ^a]	Water tagging	Length [years]
		SST	Sea ice			
LMDZ4	Present day ^b	HadISST	HadISST	353	YES	3
LMDZ4	Present day ^c	AMIP ^d	AMIP	348	YES	3
LMDZ4	SRES A1B	HadCM3	HadCM3	720	YES	3
LMDZ4	CO2 x 4	IPSL	IPSL	1392	YES	3

^a ppmv - parts per million by volume. ^b Present-day centered on 1990. ^c Present-day centered on 1992.

^d Atmospheric Model Intercomparison Project. See text for further details.

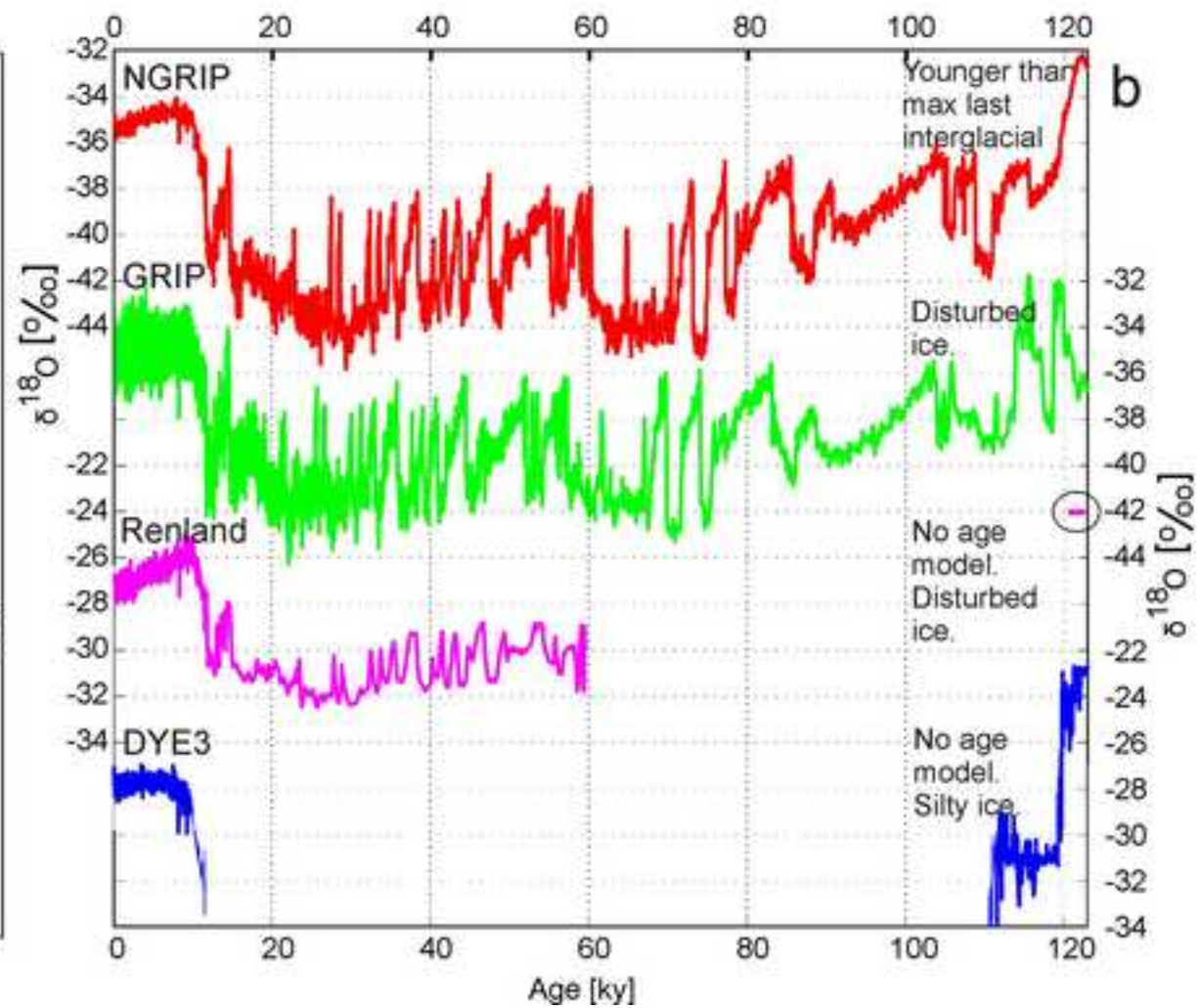
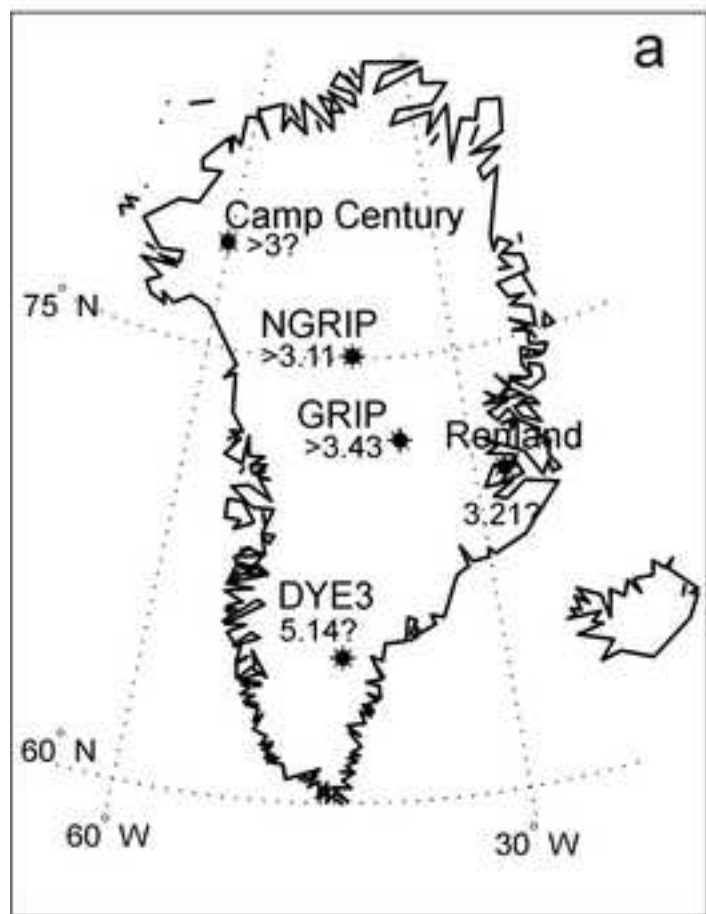
Figure C.14: Differences between the present day and SRES A1B simulations by LMDZ4 climatic and isotopic results. (a) Shading (and contouring) over Greenland shows the difference between the present day and warmer simulation values of $\delta^{18}O$ (and surface temperature) values. (b) Shading shows the $\delta^{18}O$ against temperature gradient (‰ per $^{\circ}C$) between the present day and LMDZ4 SRES A1B warmer simulation results. Contouring shows the temperature biasing (K) changes.

1100 **Appendix D. Source tracking simulations**

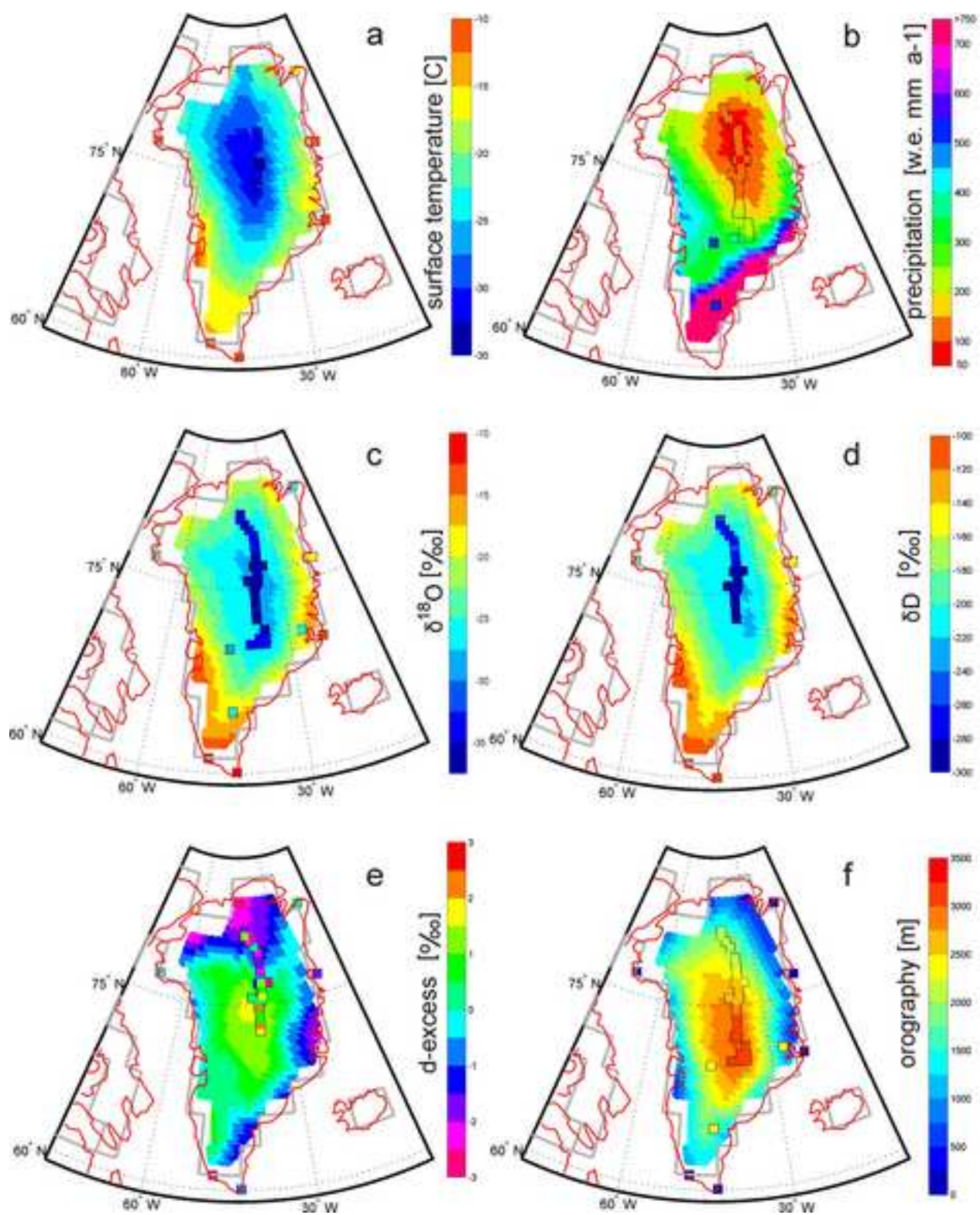
1101 In order to examine the question of precipitation sources, the same exper-
1102 iments outlined in Appendix C above, were run using the LMDZ4 source-
1103 tracking feature. Please see Risi et al. (2010), and references therein for ad-
1104 ditional details. (Note no source-tracking feature is available for HadAM3.)
1105 Using source tracking is quite computationally intensive so three years of
1106 output is used. Table 4 shows the central Greenland $\delta^{18}O$ values for the
1107 two versions of the present day simulations. Fig. D.15 shows the same re-
1108 sults, but for across the whole of Greenland, rather than for a single central
1109 Greenland average.

Figure D.15: Shading shows the mean annual $\delta^{18}O$ precipitation value associated with a given source, and contours show the percentage of precipitation associated with that particular source. Results are from the two present day experiments (left panels) HadAM3 present-day, and (right panels) LMDZ4 present day. Source regions are: (a,b) all sourced regions; no precipitation contours given because all values are 100%; (c,d) high-latitude (north of $50^\circ N$) sea surface areas, (e,f) mid-low latitude (south of $50^\circ N$) sea surface areas, and (g,h) continental (all non-sea surface).

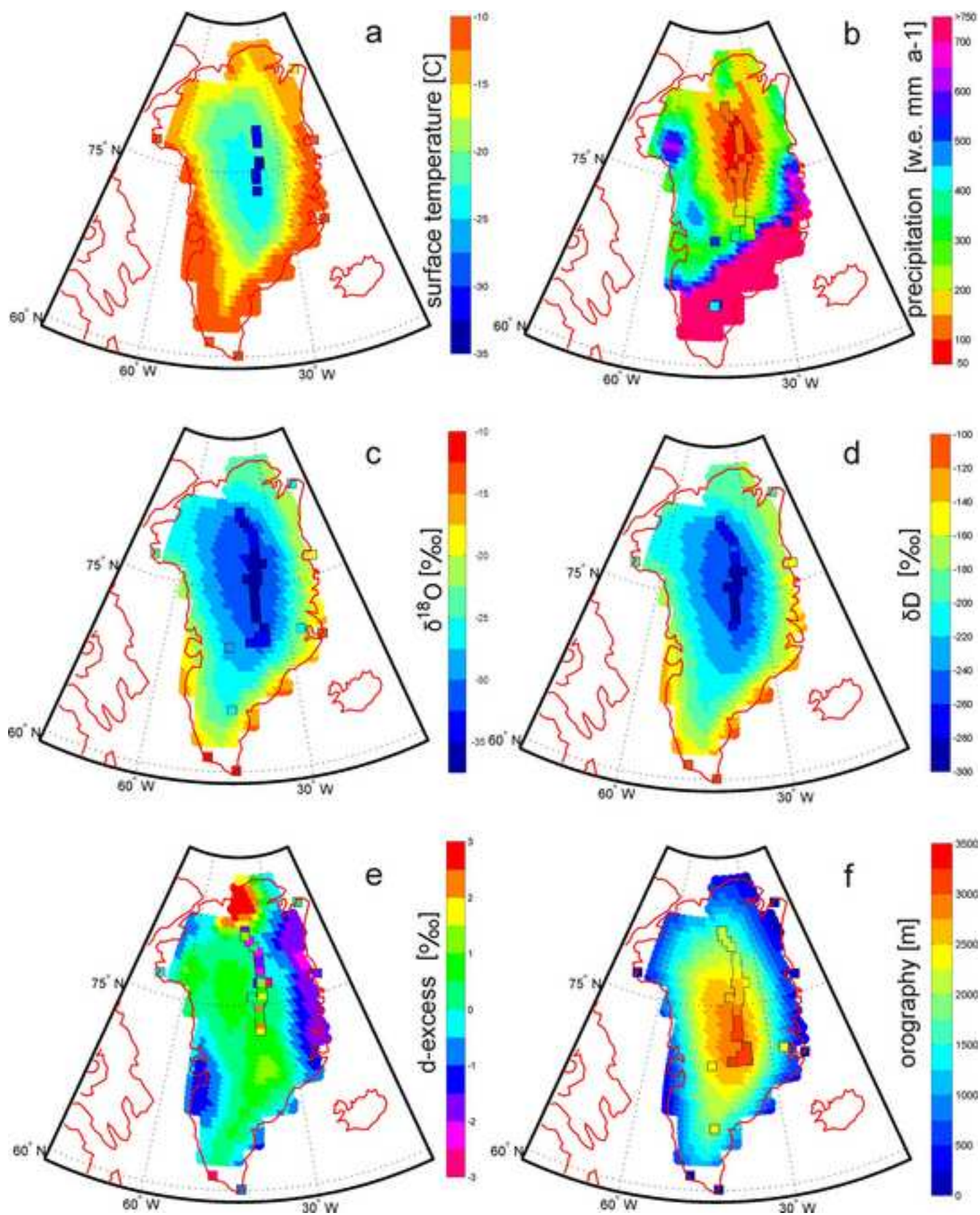
*Figure
[Click here to download high resolution image](#)



*Figure
[Click here to download high resolution image](#)



*Figure
[Click here to download high resolution image](#)



*Figure

[Click here to download high resolution image](#)

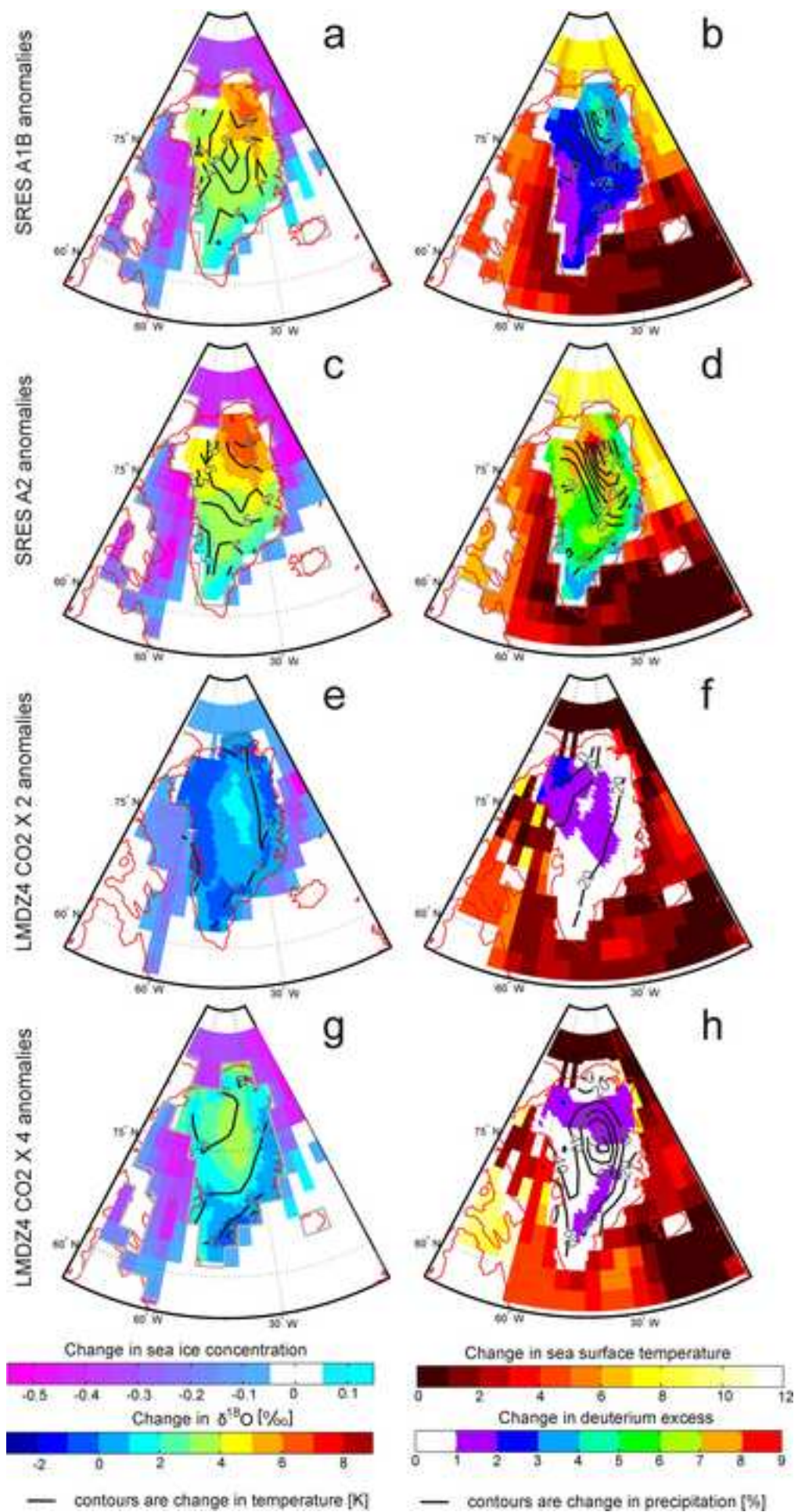


*Figure
[Click here to download high resolution image](#)

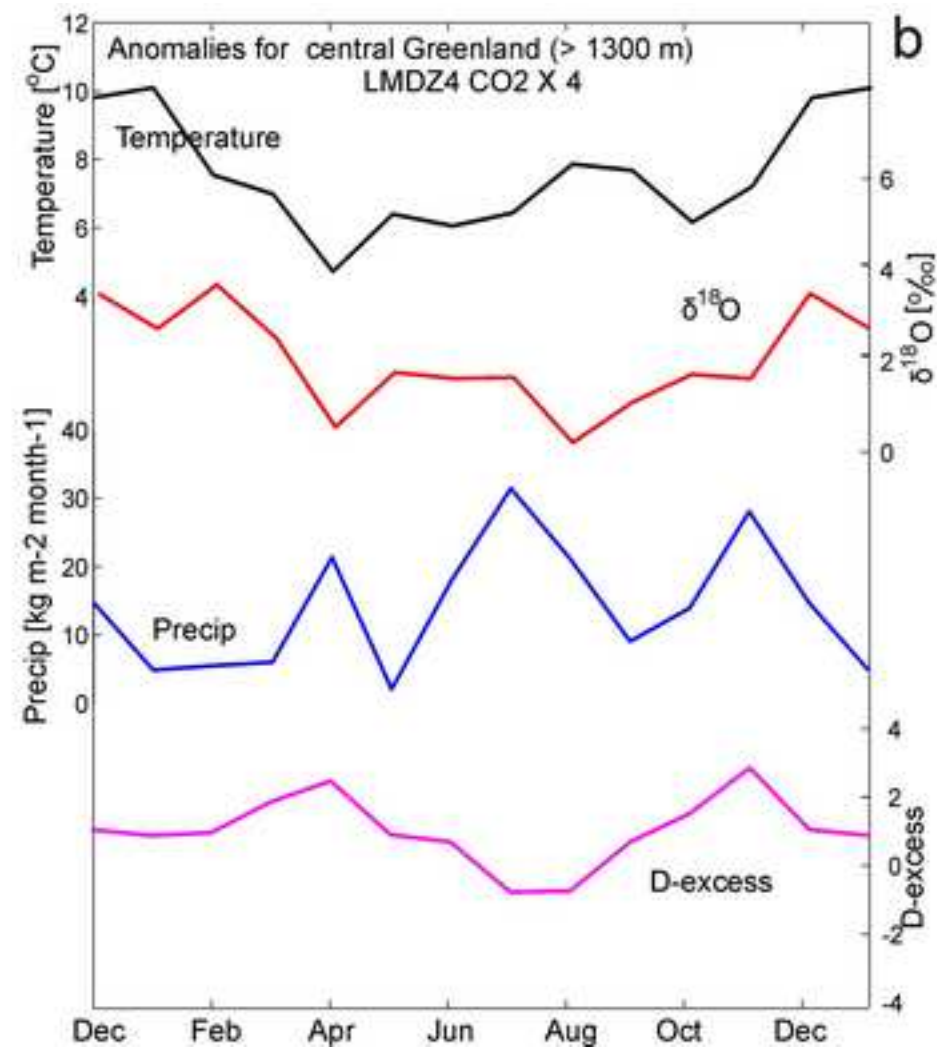
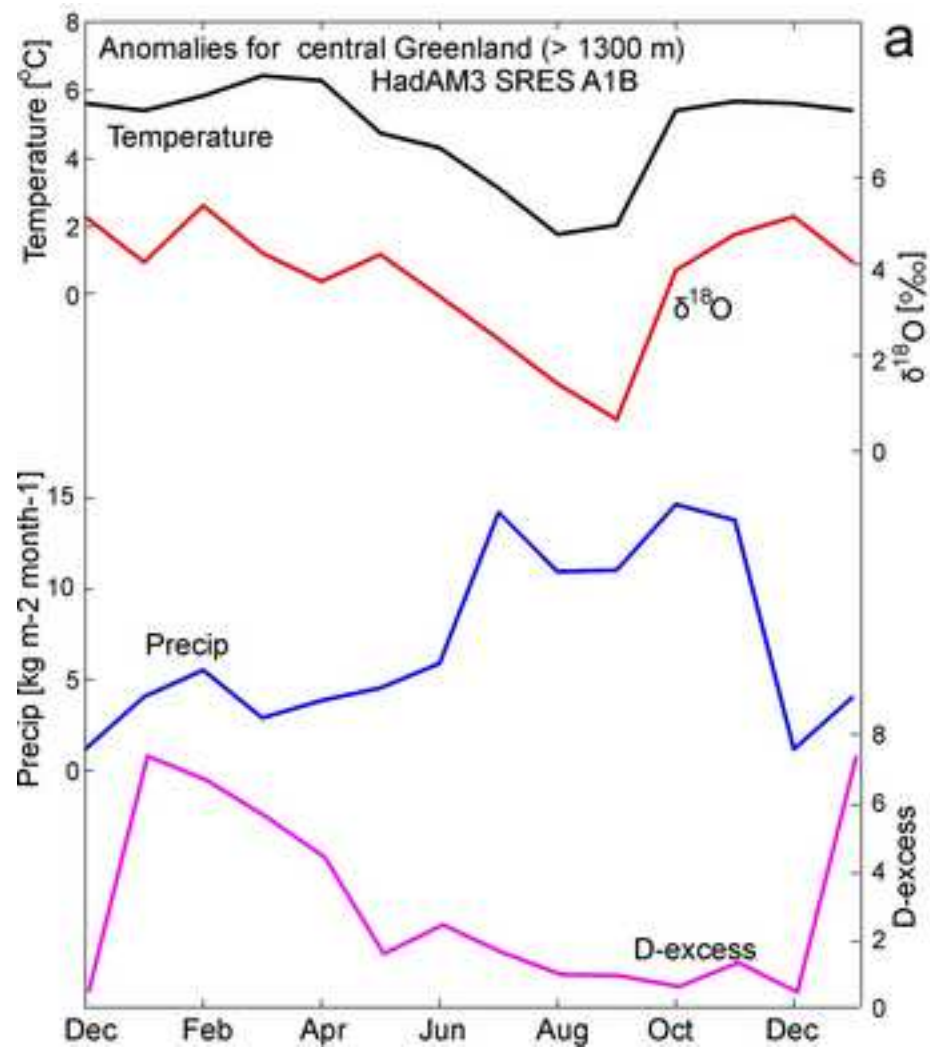
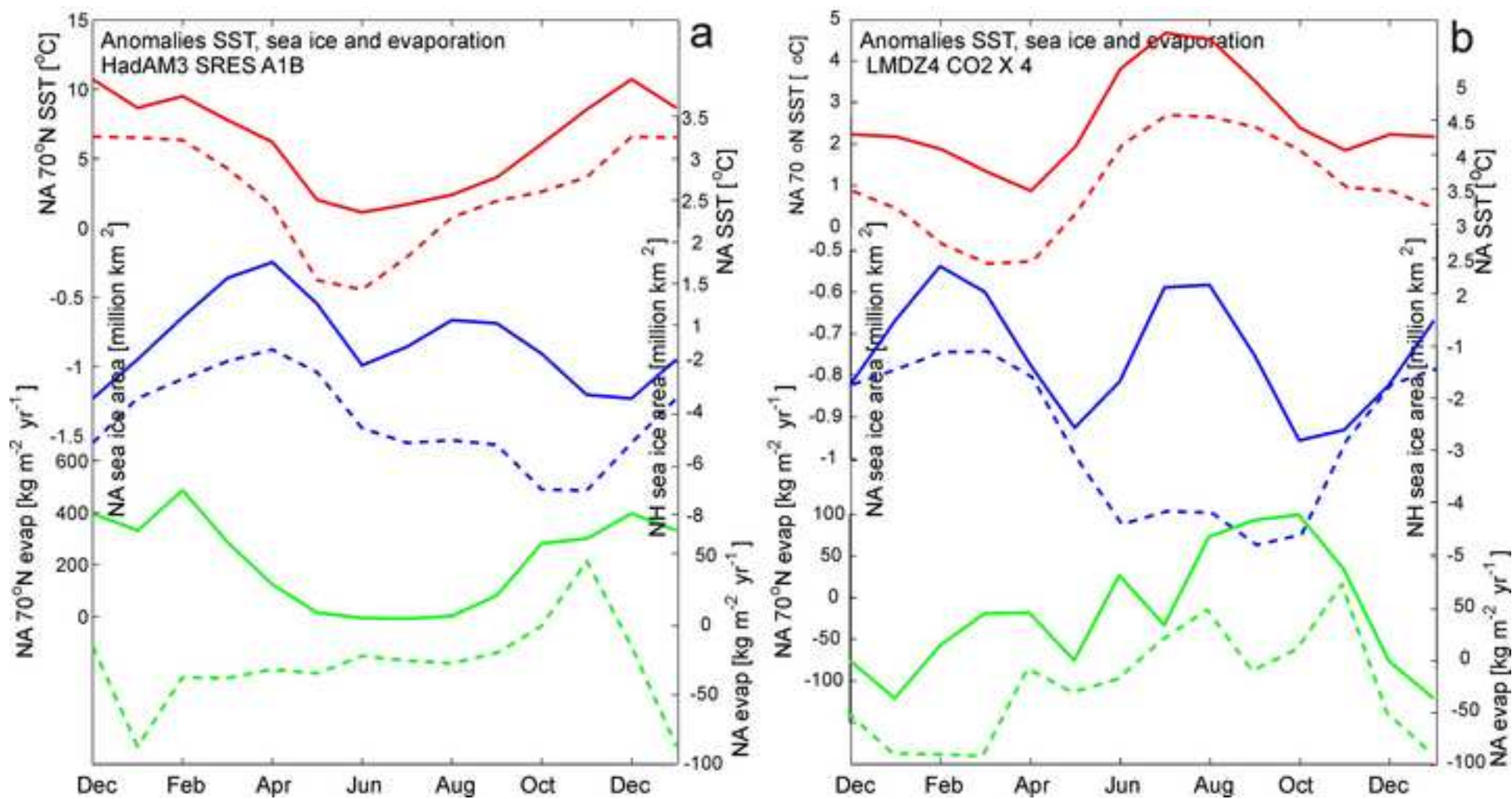
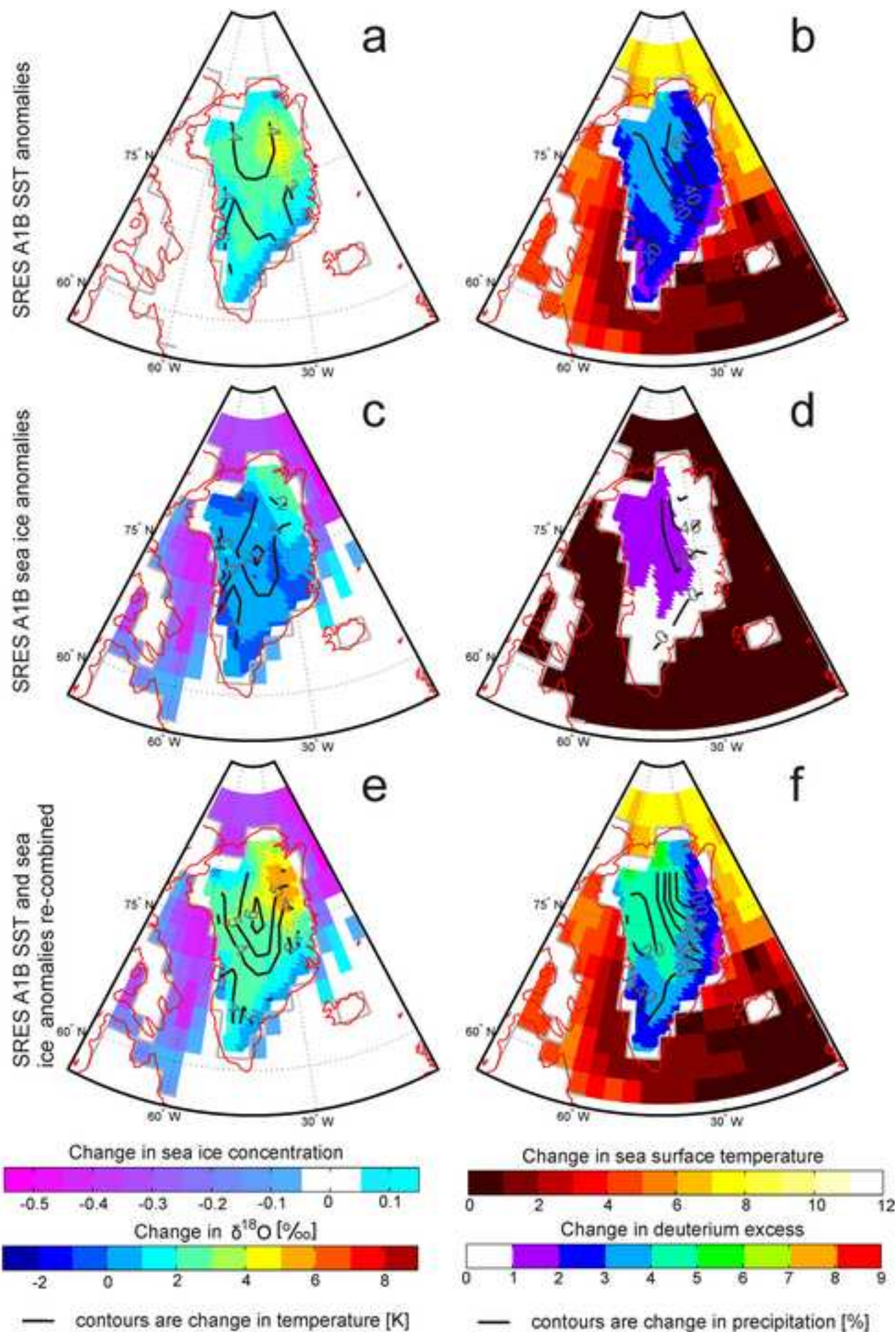


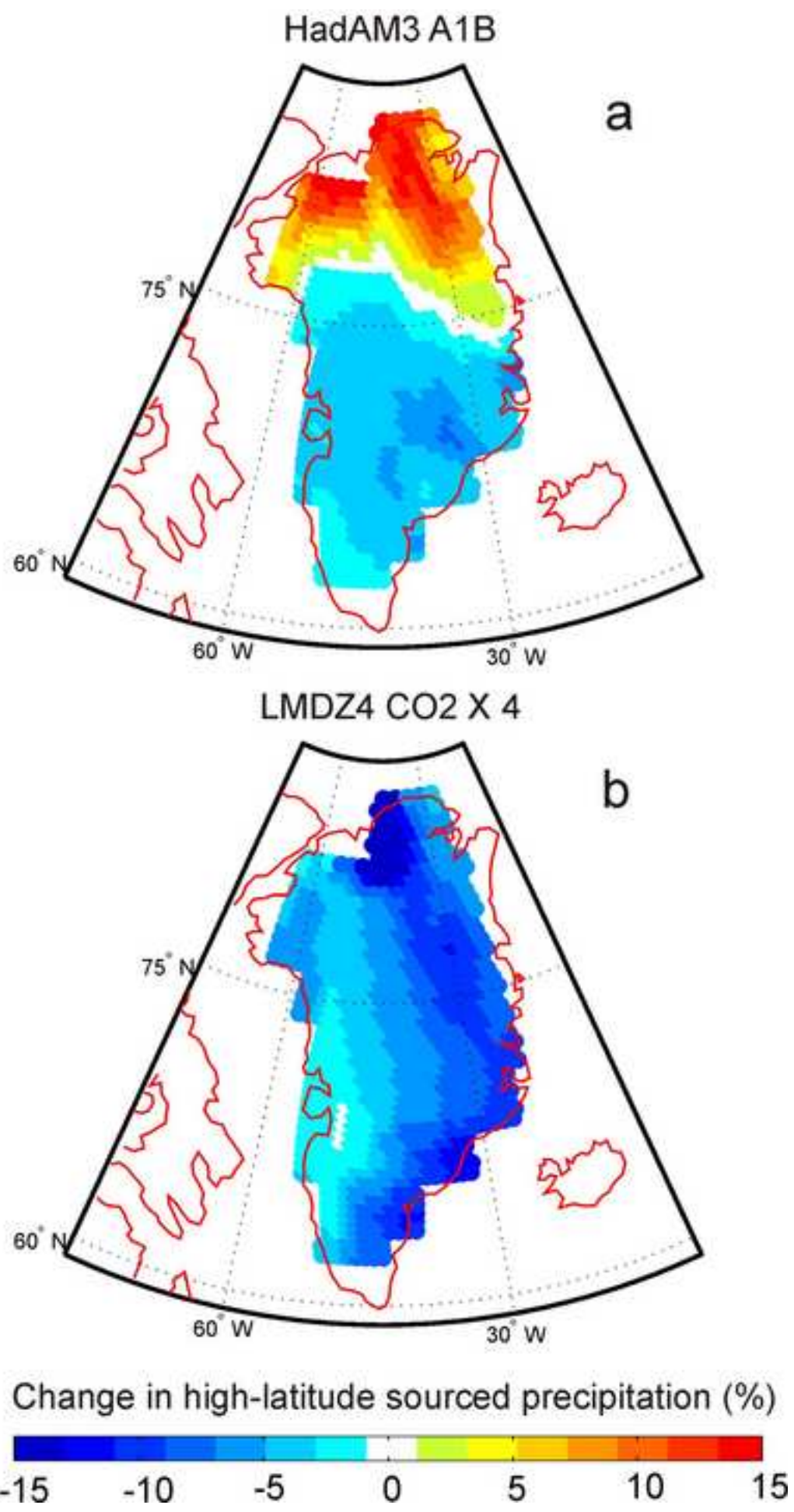
*Figure
[Click here to download high resolution image](#)



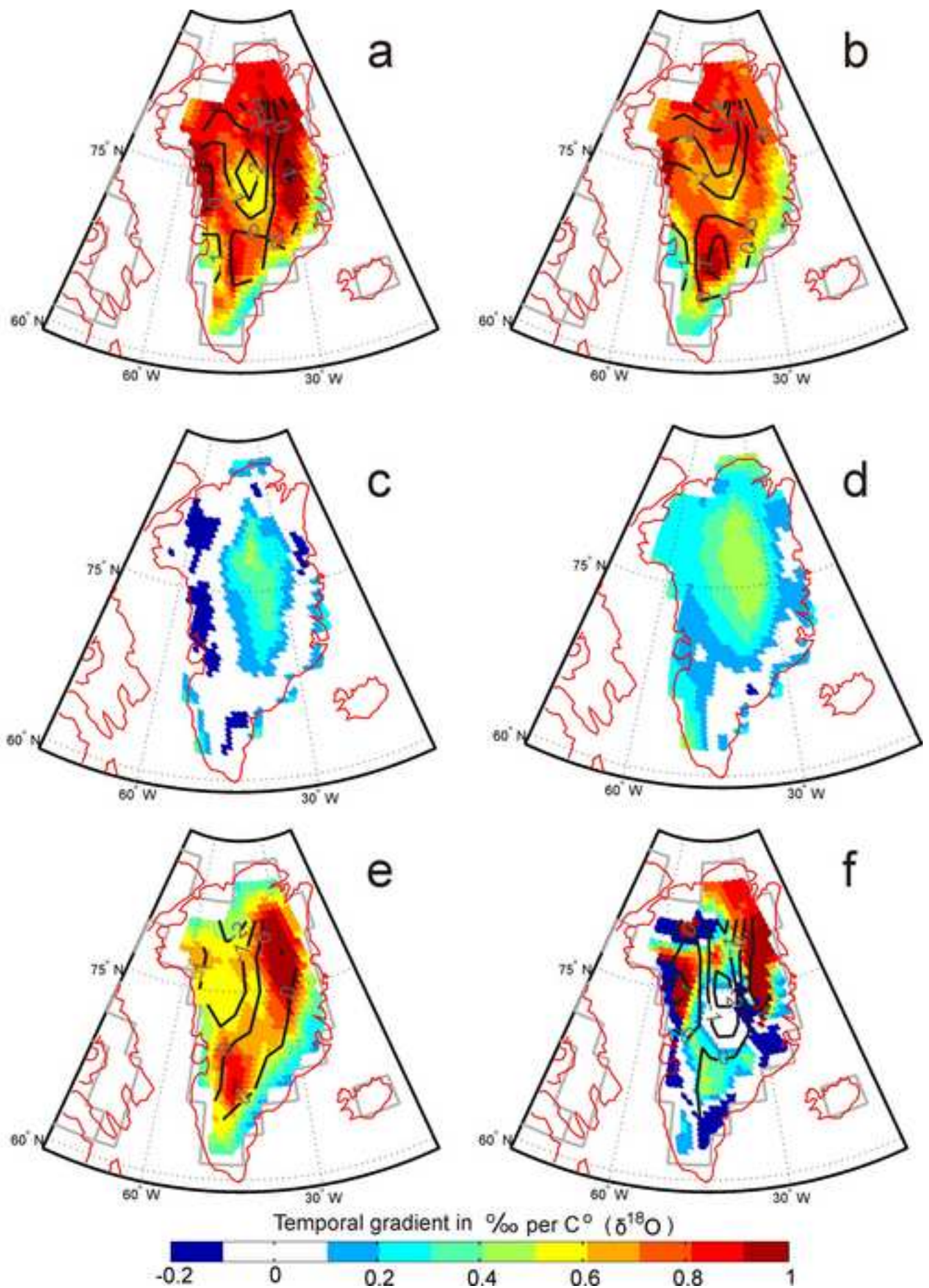
*Figure

[Click here to download high resolution image](#)





*Figure
[Click here to download high resolution image](#)



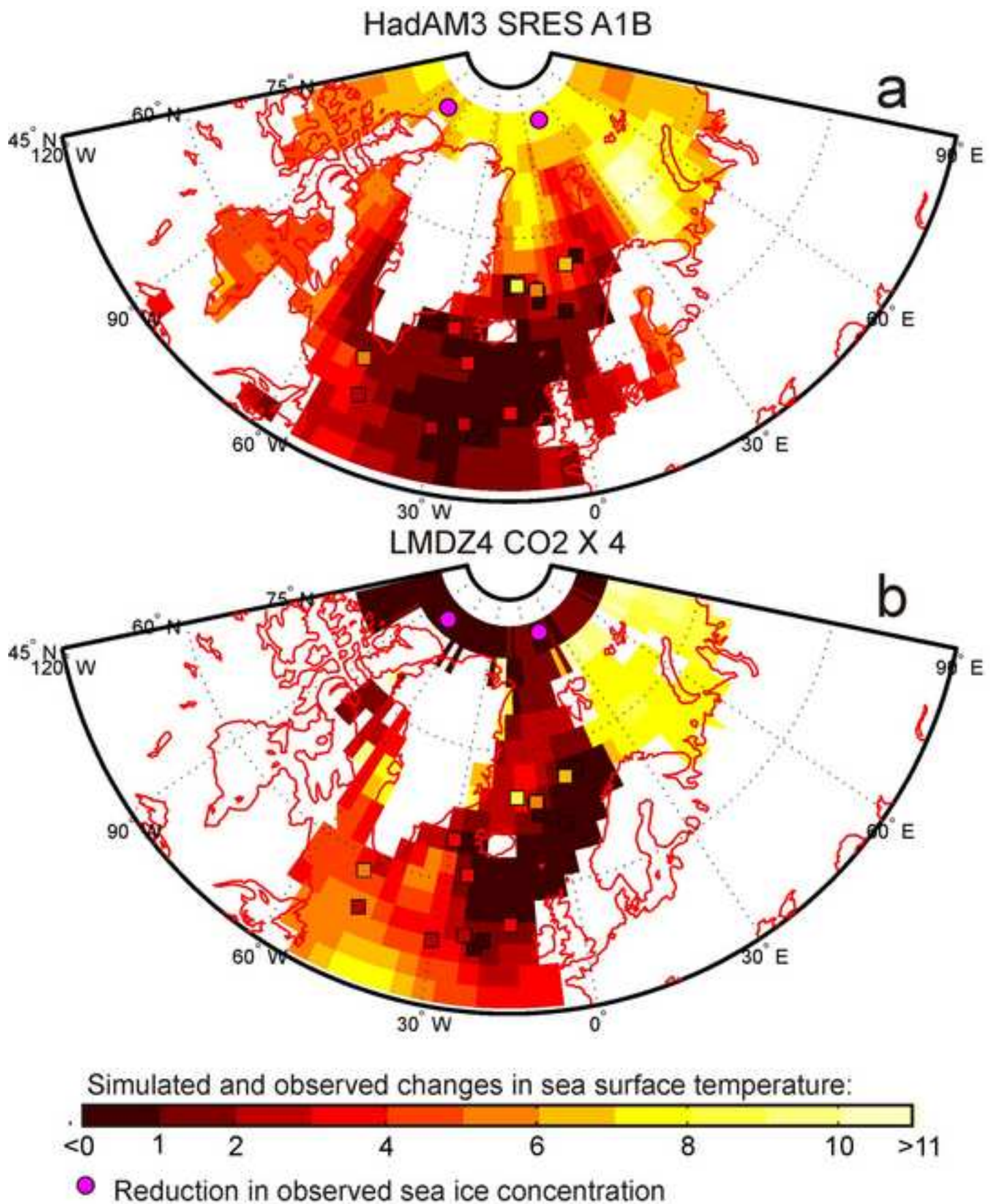


*Figure
[Click here to download high resolution image](#)

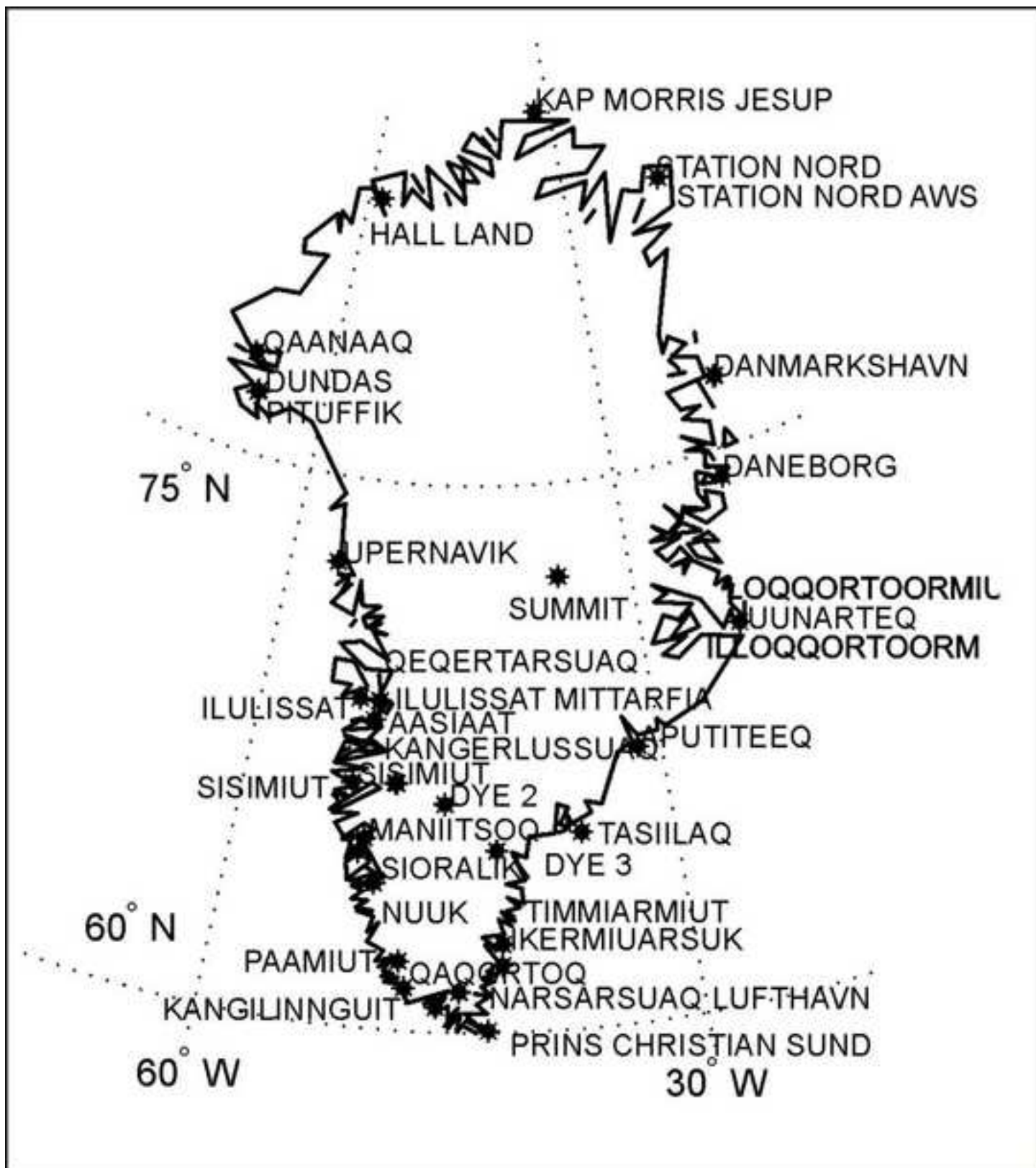


*Figure
[Click here to download high resolution image](#)

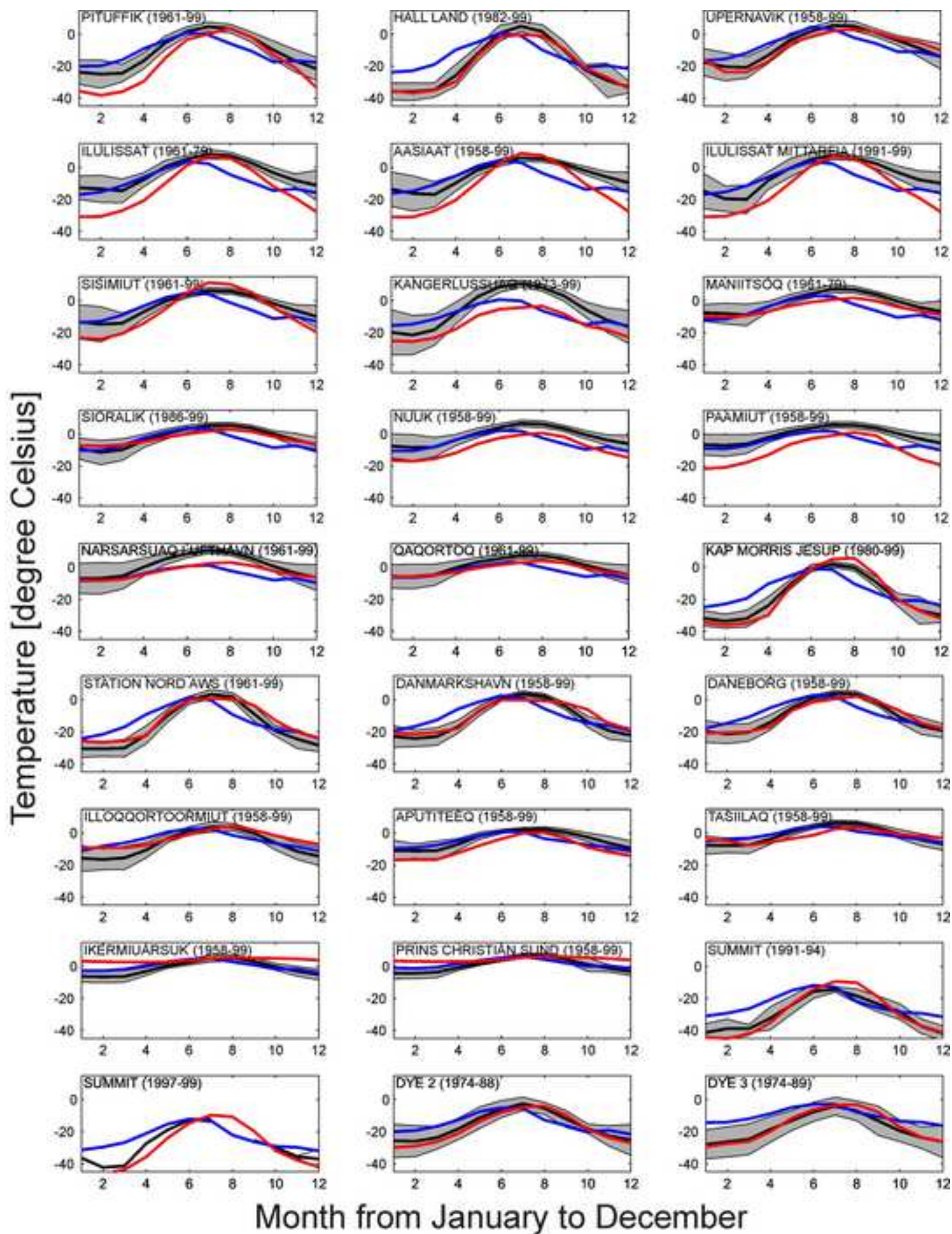


*Figure
[Click here to download high resolution image](#)

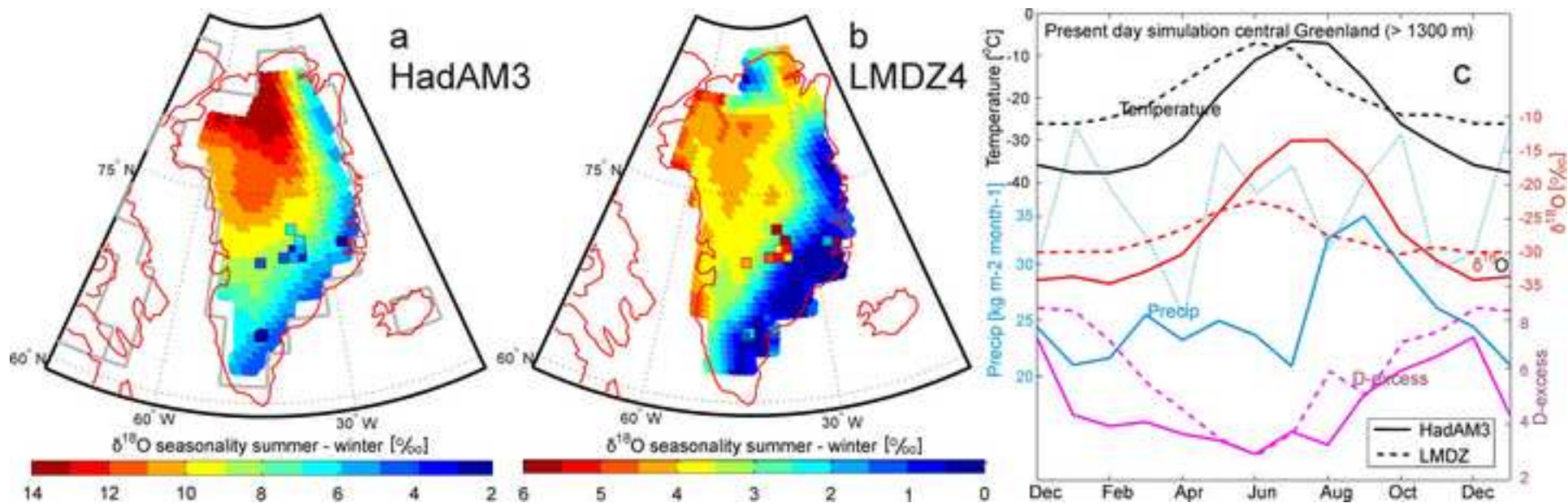


*Figure
[Click here to download high resolution image](#)

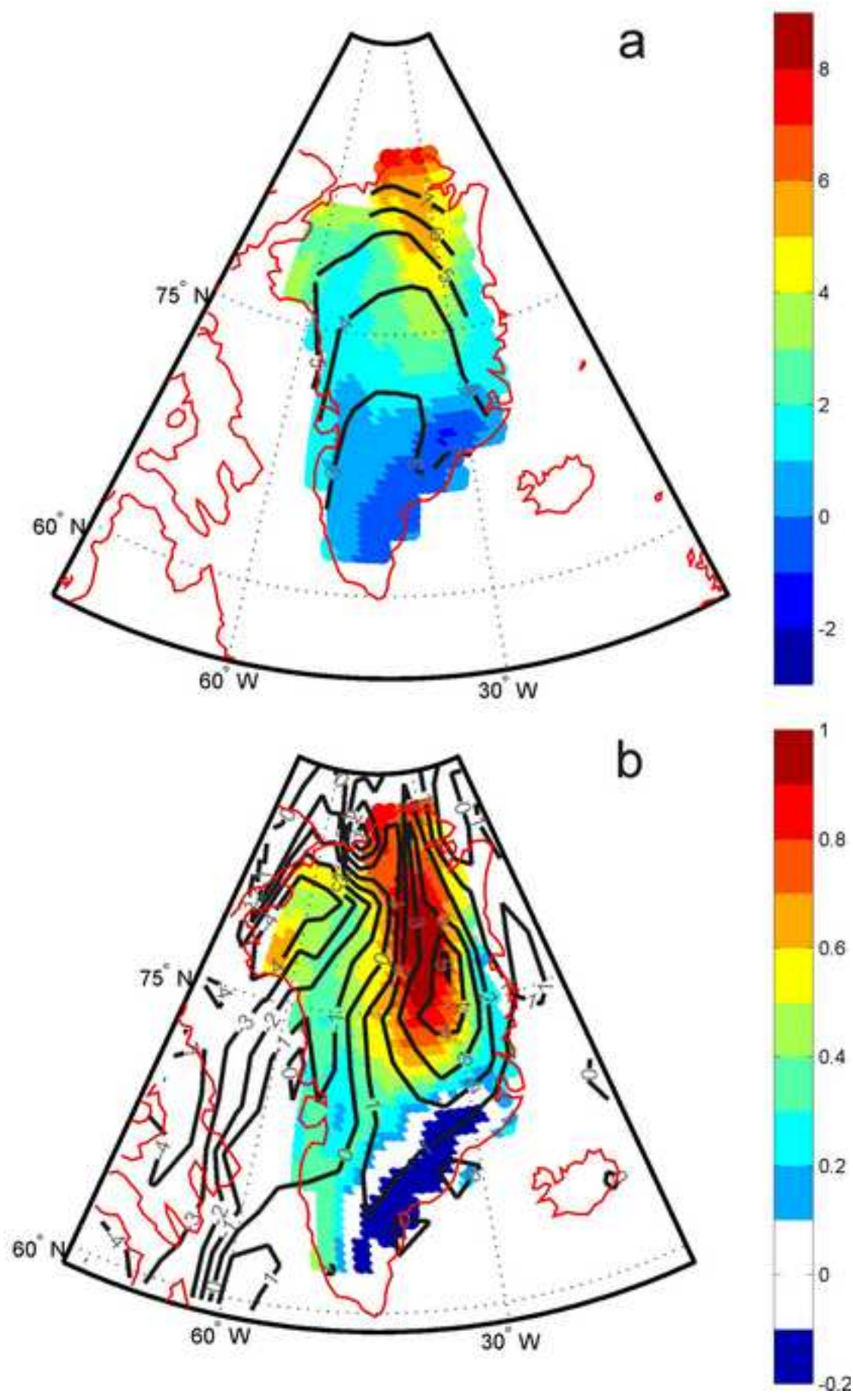


***Figure**
[Click here to download high resolution image](#)

